

FAST X-RAY IMAGING AND DIFFRACTION FOR **ENGINEERING MATERIALS SCIENCE**

Tao Sun

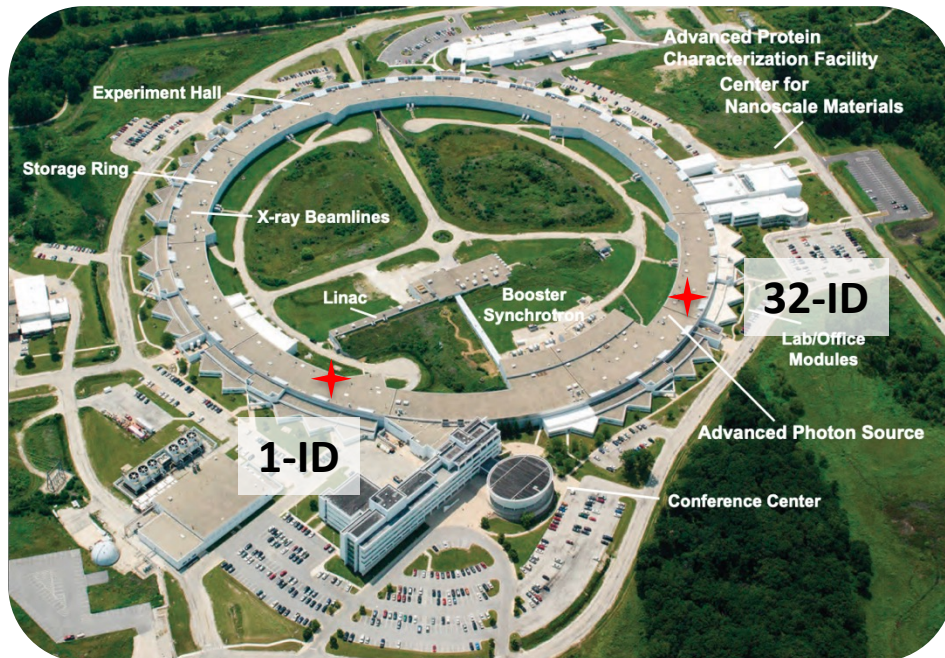
Department of Materials Science and Engineering

University of Virginia

24th National School on Neutron and X-Ray Scattering
July 19, 2022



Contents



- I. High-speed x-ray imaging at 32-ID-B beamline of Advanced Photon Source
- II. Operando synchrotron experiments on metal additive manufacturing
- III. Fast diffraction experiments at different time scales (32-ID vs 1-ID)

32-ID: Dr. Kamel Fezzaa and Dr. Samuel Clarke
1-ID: Dr. Andrew Chuang

QUESTIONS WE WILL ANSWER TODAY

- 1) What is special about engineering materials science?**
- 2) What are the main advantages of synchrotron over lab-source?**
- 3) What make APS an unique facility for high-speed x-ray experiments?**
- 4) What affect the spatial and temporal resolutions of the imaging experiment?**
- 5) How to choose different in situ diffraction techniques?**

“FAST” ENGINEERING MATERIALS SCIENCE

Real materials under real conditions in real time

- Millimeter sample size to represent bulk behavior
- Complex system to deliver realistic work conditions

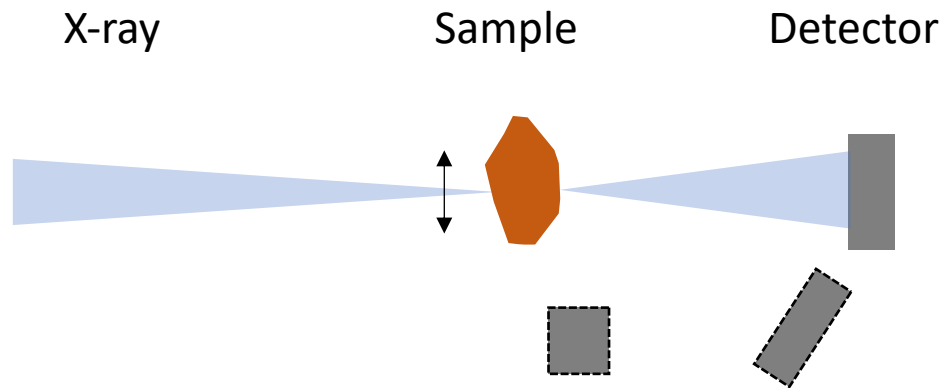
- Fluid dynamics
- Energetic materials and rapid reactions
- Dynamic loading
- Materials machining and processing
- Additive manufacturing

Dynamic irreversible and non-repeatable materials and engineering processes



X-RAY IMAGING AND MICROSCOPY TECHNIQUES

□ Scanning probe microscopy



- Fluorescence contrast
- Absorption contrast
- Absorption fine structure contrast
- Scattering contrast
- Diffraction contrast
- Computed tomography (3D)

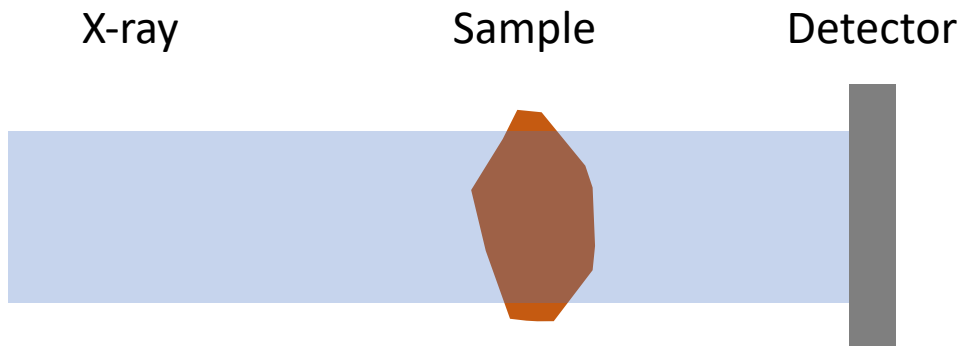
*Spatial resolution:
probe size*

□ Coherent imaging

- Ptychography
- Coherent diffractive imaging

*Spatial resolution:
q range*

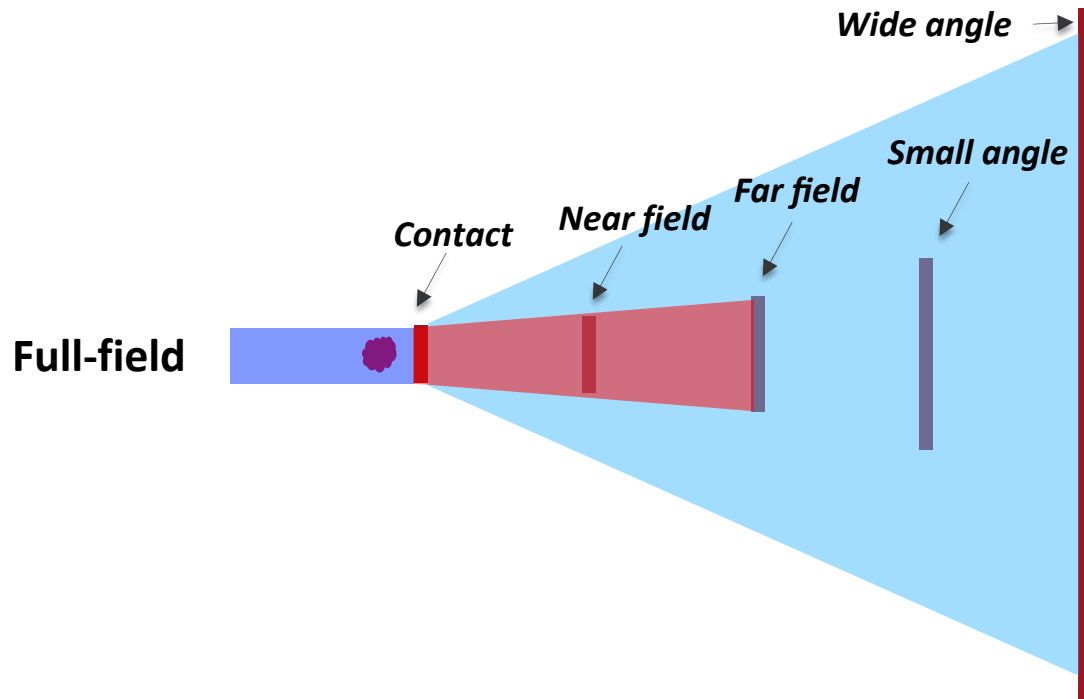
□ Propagation-based full-field imaging



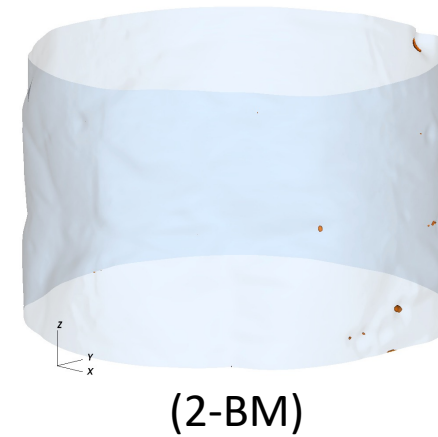
- Absorption contrast
- Phase contrast imaging
- Projection microscopy
- Transmission x-ray microscopy
- Diffraction contrast
- Computed tomography (3D)

*Spatial resolution:
detection pixel size*

PROPAGATION-BASED FULL-FIELD X-RAY IMAGING



3D reconstruction



X-ray micro computed tomography

Transmission x-ray microscope (x-ray nano CT)

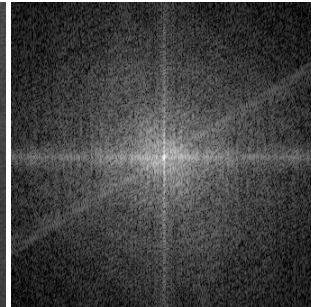
Absorption contrast imaging



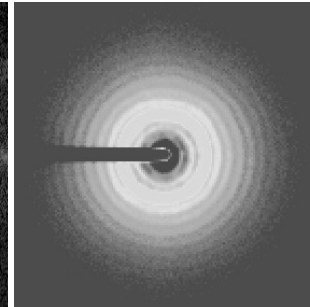
Phase contrast imaging



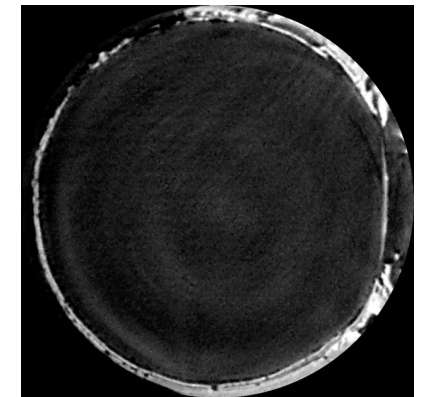
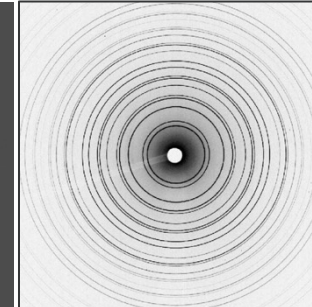
Coherent diffractive imaging



Small-angle scattering

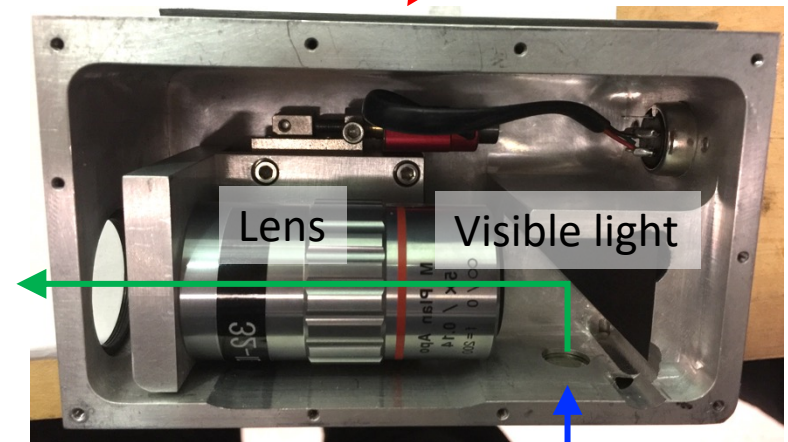
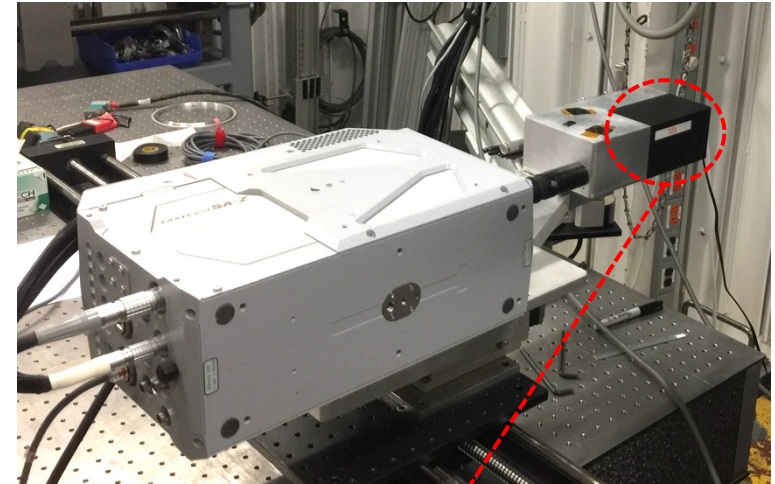
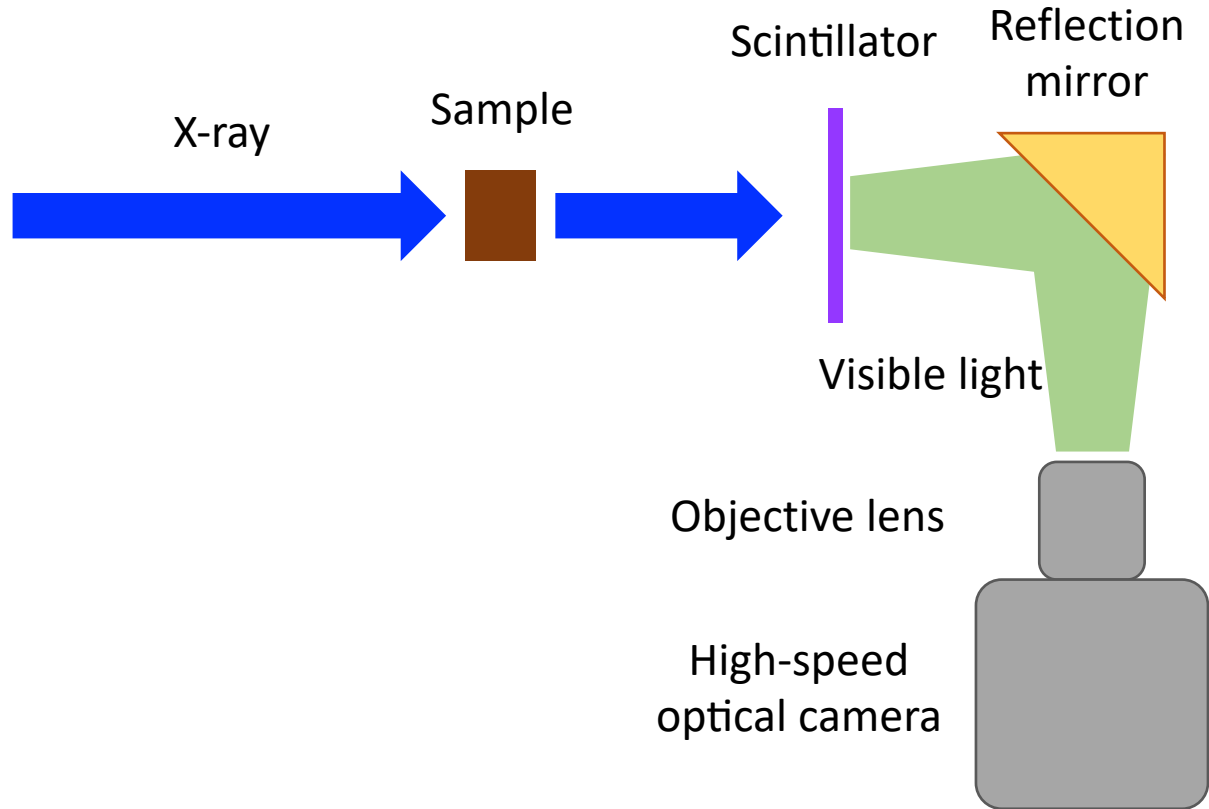


Diffraction or wide-angle scattering



(32-ID-C)

HIGH-SPEED X-RAY IMAGE DETECTION SYSTEM



Scintillator-couple optical detection

- High spatial resolution: imaging sensor pixel size, magnification by the lens
- High temporal resolution: delay time of scintillator, frame rate and exposure time of camera, x-ray pulse structure

SPATIAL RESOLUTION

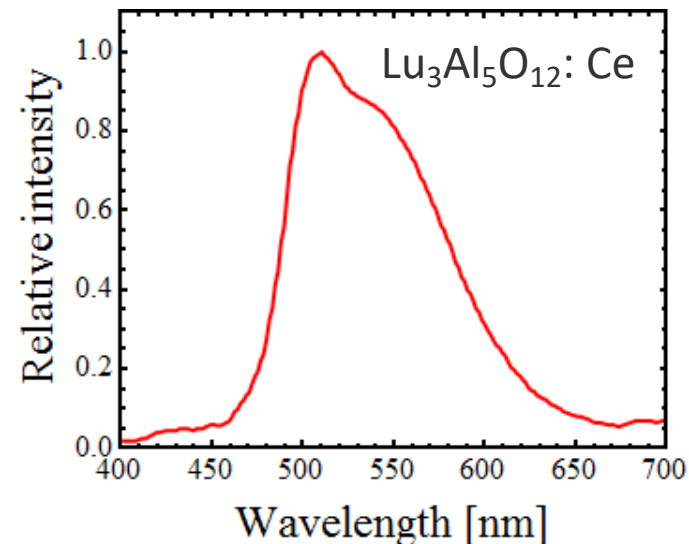
- ❑ X-ray beam size: 2 mm x 2 mm
- ❑ Camera sensor:
 - CMOS: 20 μm /pixel, 1024 x 1024, image size reduces as frame rate increases
 - Hybrid CMOS (with on-pixel storage): 30 μm /pixel, 400 x 250, image size remains the same
- ❑ Objective lens: 2x, 5x, 10x, 20x
- ❑ Scintillator light emission: visible light (wavelength: 400~700 nm)



Photron FastCam SA-Z



Shimadzu HPV-X2



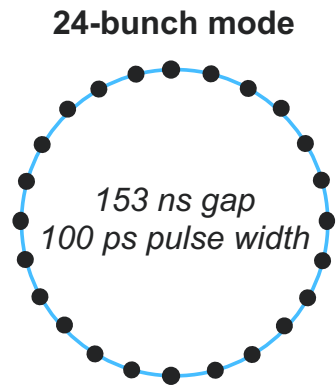
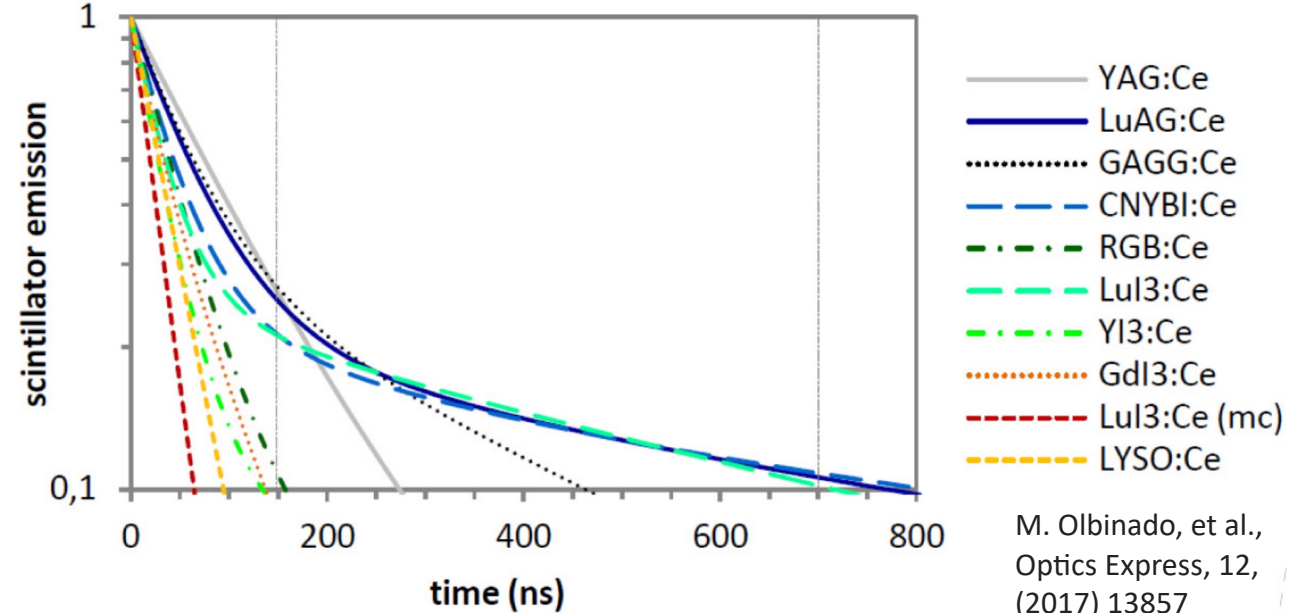
TEMPORAL RESOLUTION

❑ Exposure time:

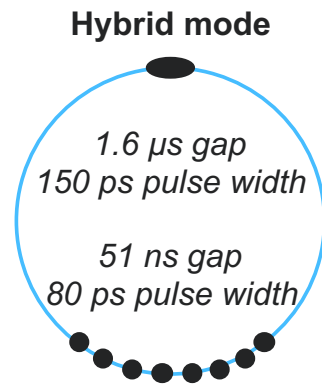
- Camera specs (CMOS: 100s' ns; Hybrid-CMOS: 50 ns)
- Scintillator decay time

❑ Frame rate:

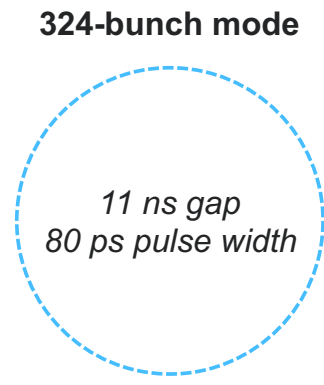
- Camera specs (CMOS: 1 MHz; Hybrid-CMOS: 10 MHz)
- Needed field-of-view for experiment
- X-ray pulse structures



6.5
MHz



271 kHz
(19.6MHz)



87.8 MHz

24-bunch mode: MHz imaging with single pulse exposure

Hybrid mode: Fixed frame rates, but stronger single pulse

324-bunch mode: Experiments with $> \mu$ s exposure, no intensity fluctuation in each image

32-ID BEAMLINE UNDULATOR SOURCES

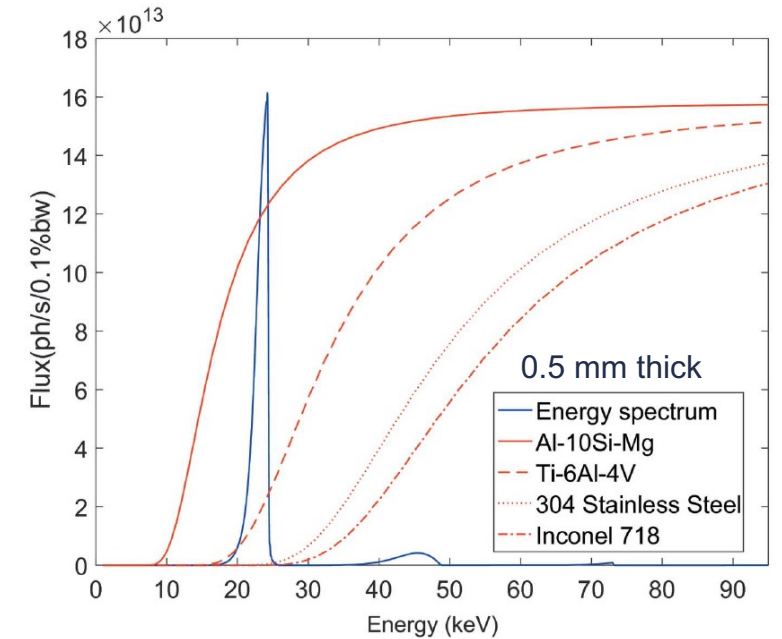
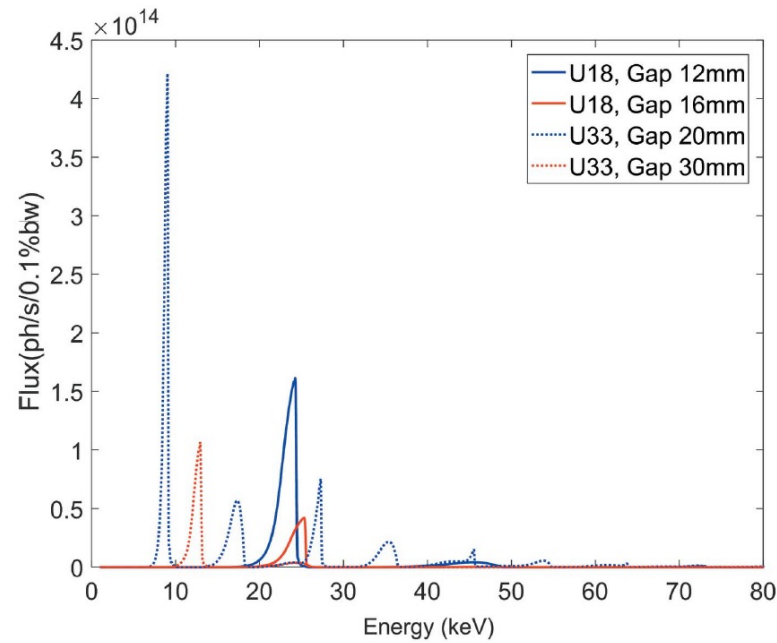
Tandem undulators

☐ U33 (white beam)

- Length: 2.4 m
- Period: 3.3 cm
- Min Gap: 11 mm
- E1 range: 5~14 keV
- $\Delta E_1/E_1$: 1~2%

☐ U18 (pseudo pink beam)

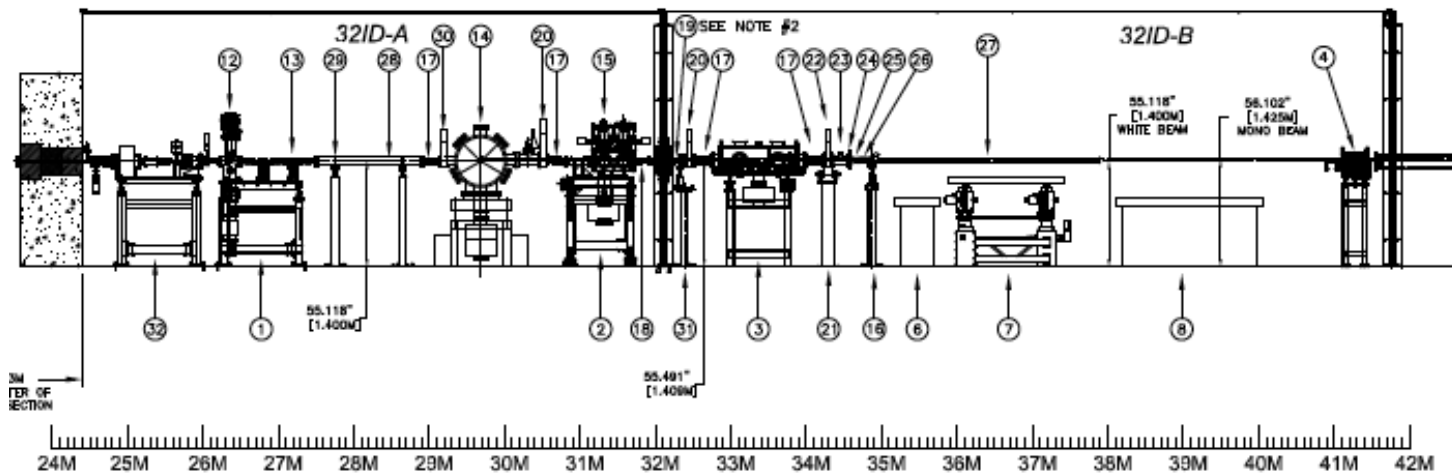
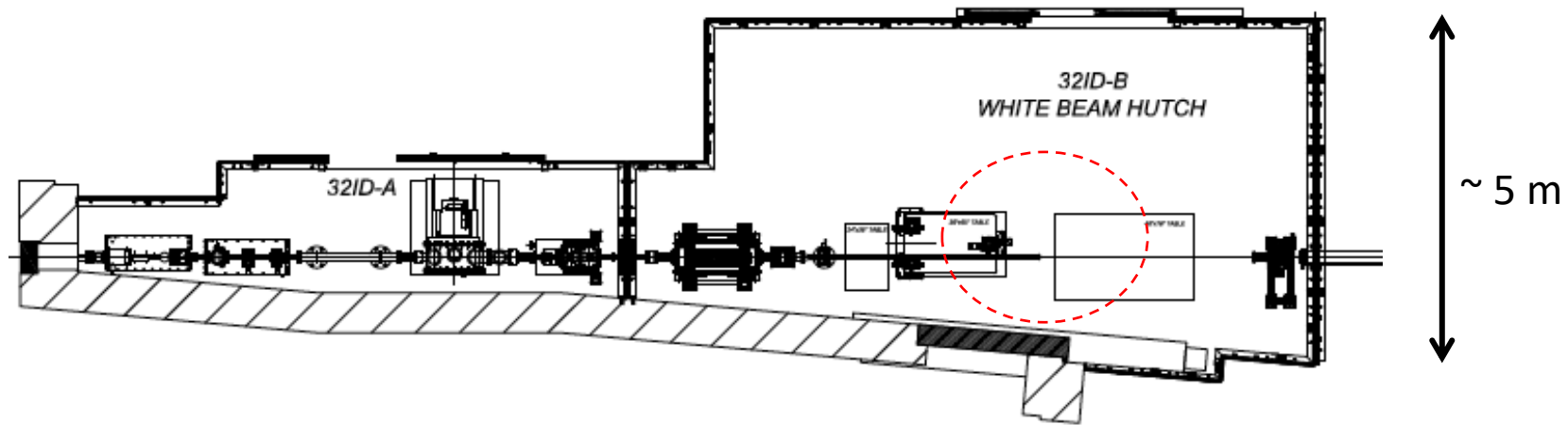
- Length: 2.4 m
- Period: 1.8 cm
- Min Gap: 11 mm
- E₁ range: 23.7~25.7 keV
- $\Delta E_1/E_1$: 5~10%



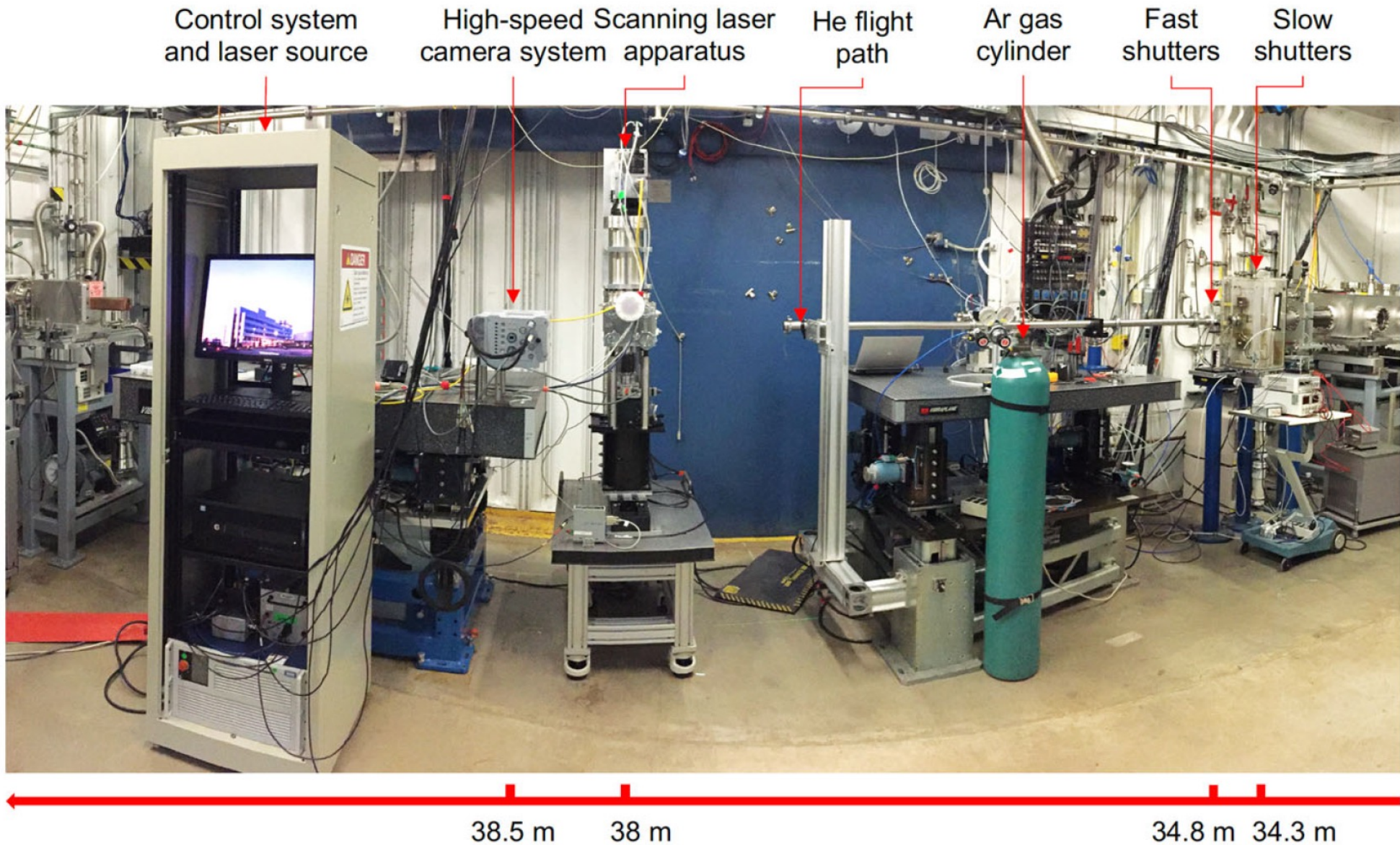
Undulator		Integrated over 1-65 keV		1st harmonic	
Period (cm)	Gap(mm)	Flux*	Singlet	Flux	Singlet
3.3	20	1.8×10^{16}	2.8×10^9	1.3×10^{16}	2.0×10^9 (71%)
	30	4.7×10^{15}	7.3×10^8	4.5×10^{15}	6.9×10^8 (95%)
1.8	11	4.5×10^{16}	6.9×10^9	4.1×10^{16}	6.3×10^9 (92%)

* Unit: ph/s/0.1%BW, 1.5x1.5 mm² beam size

32-ID-B EXPERIMENTAL HUTCH

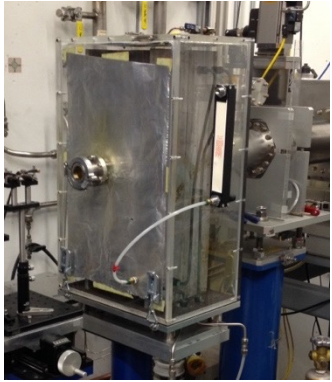


32-ID-B EXPERIMENTAL HUTCH

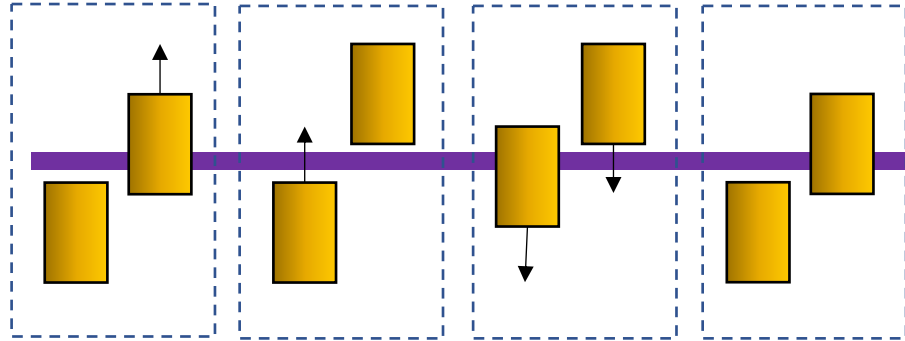


TIMING SCHEME AND BEAMLINE CONTROL

Slow shutters



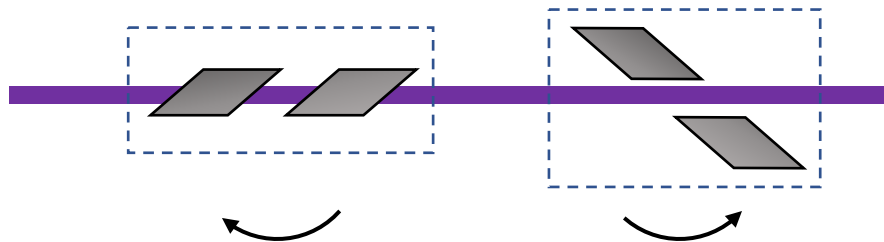
Opening — 50 ms — Closing



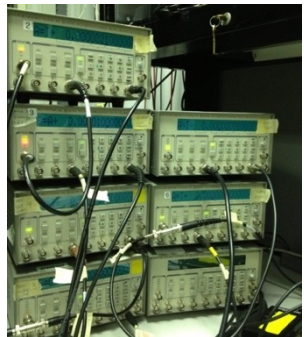
Fast shutters



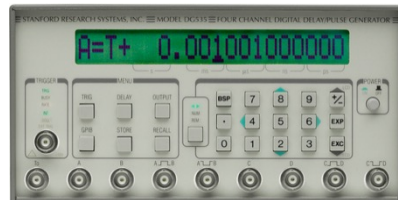
Close — 700 μ s — Open



Delay generators



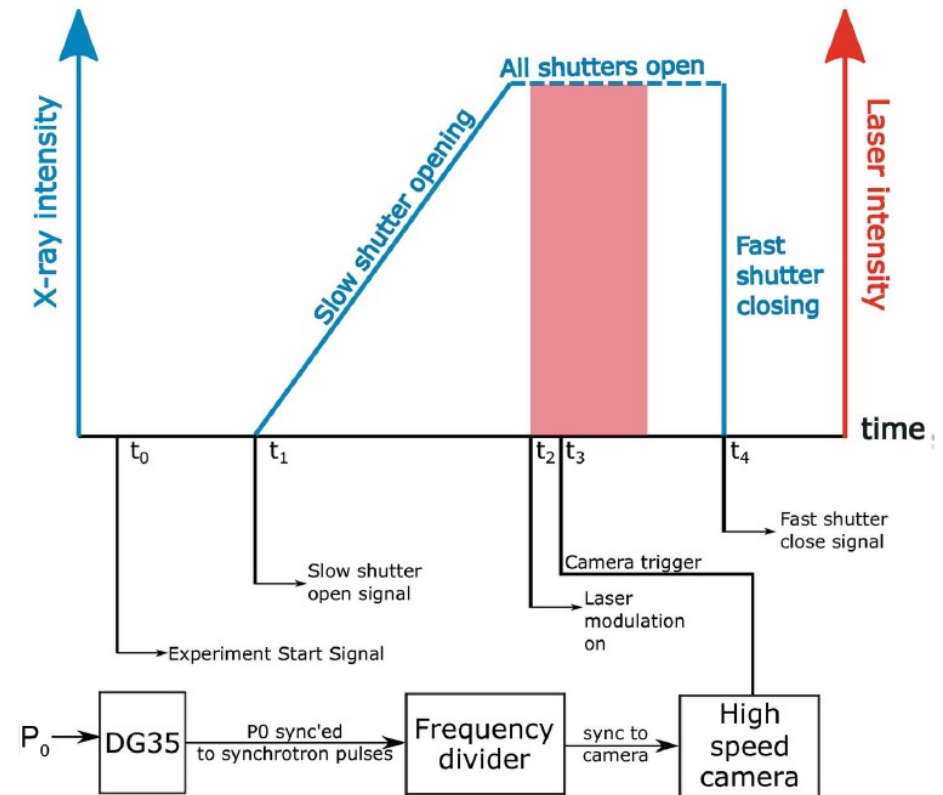
SRS535



SRS645



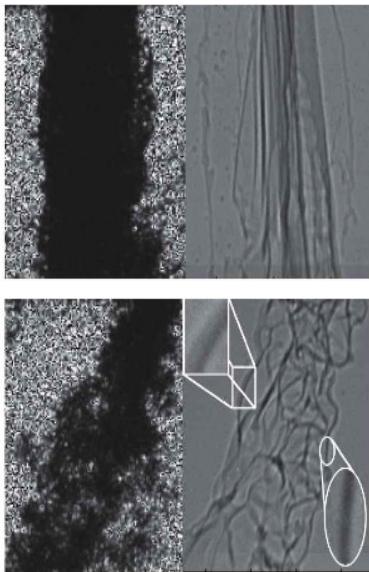
Timing scheme



“FAST” ENGINEERING MATERIALS SCIENCE



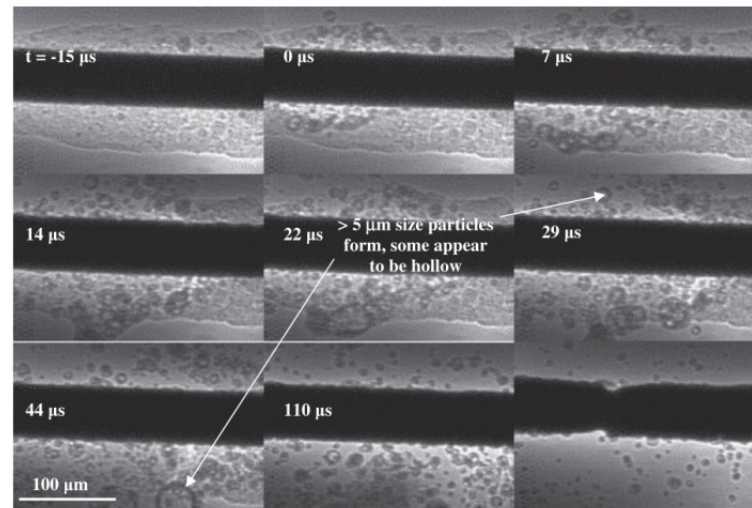
Fuel spray: visible light vs X-ray



Wang Y. et al. Nature Physics 4, 305-309 (2008)



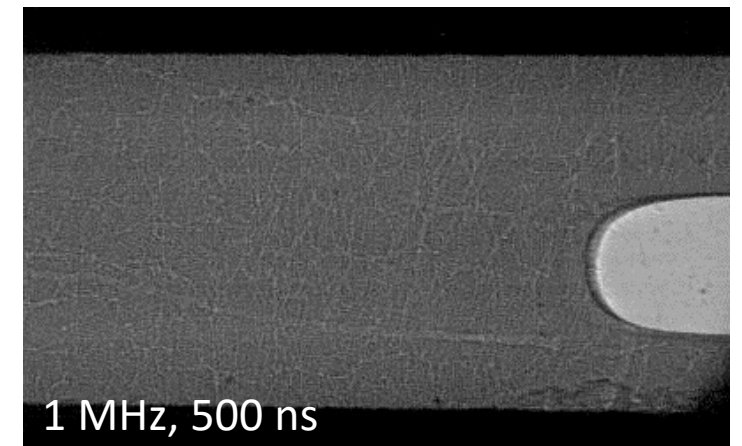
Thermite reaction: Al-Fe₂O₃



K. Sullivan et al. Combustion and Flames 159, 2-15 (2012)



Fracture of bone upon impact



From Wayne Chen's group, Purdue University

METAL ADDITIVE MANUFACTURING

Basics of additive manufacturing technologies (3D printing)

❑ Build parts layer by layer

- Digital manufacturing nature
- Parts with complex geometries
- Highly customized components
- On site and on demand build
- Short supply chain and easy stock management
- Potentially energy and material saving

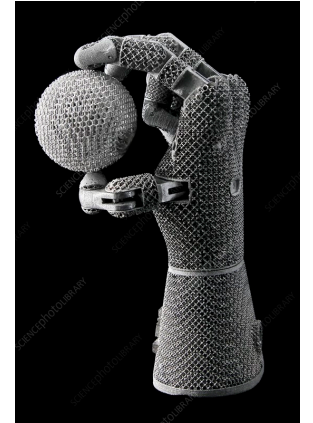
❑ Been around for > 30 years: from rapid prototyping and tooling to end-use product manufacturing

❑ Recent surge of popularity was driven by

- Expiration of a few key patents
- Advance of computer hardware and software
- Reduced cost of key components, e.g. laser source
- Need for complex parts with improved performance in many industries
- Need for secure supply chain

Complex objects

Engine nozzle



Heat exchanger



Piston

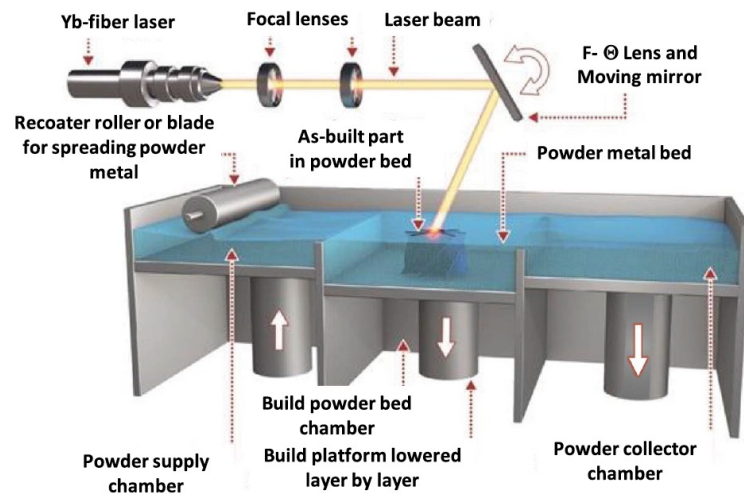


Implant



METAL ADDITIVE MANUFACTURING

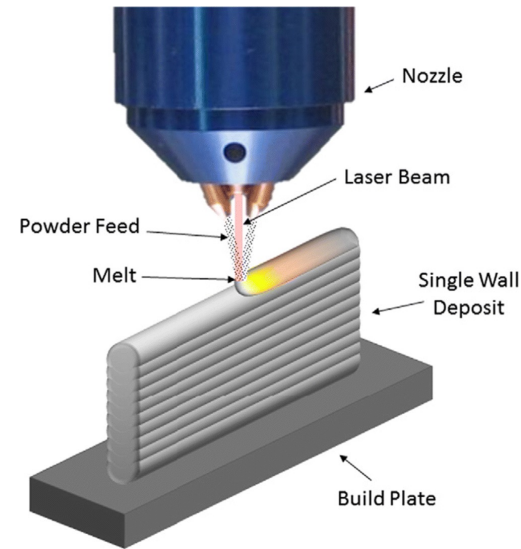
Laser powder bed fusion



T. Özel, et al., Journal of Manufacturing Science and Engineering, 142, (2020) 011008

- Powder bed
- Scanning laser melting
- Electron beam technique: electron beam melting (EBM)

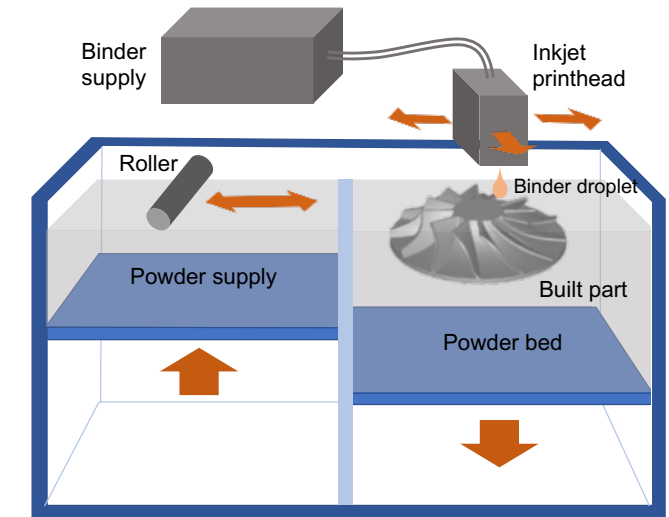
Directed energy deposition



A. Reichardt, et al., Materials & Design, 104, (2016)

- Printhead with heat source and feedstock built in
- Heat source: laser or electron beam
- Feedstock: powder and wire

Binder jetting



- Powder bed
- Liquid binder “gluing”
- All type of materials
- Print + sintering

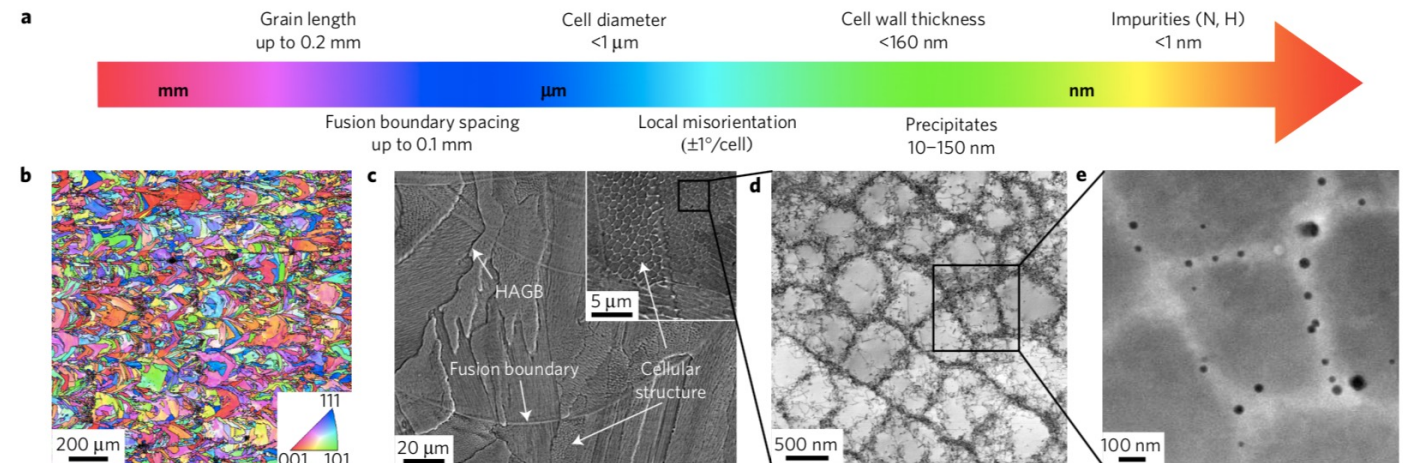
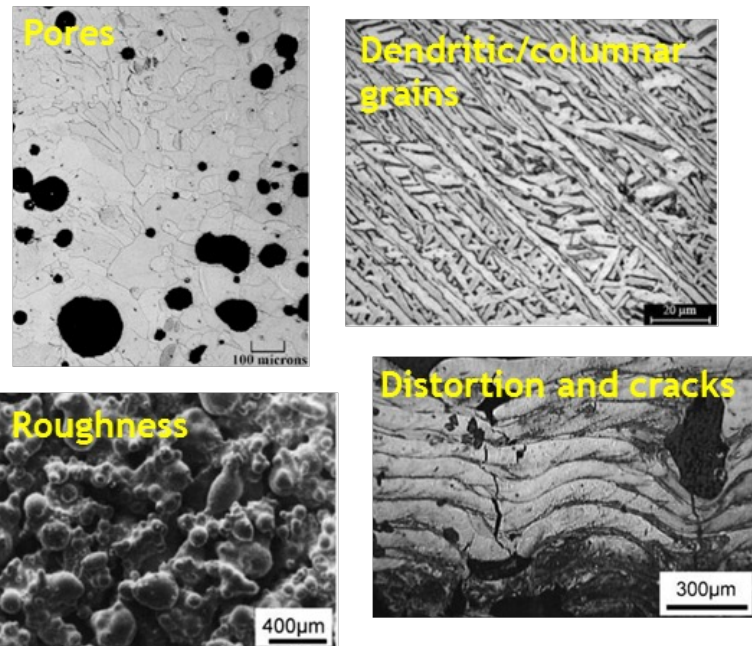
CURRENT PROBLEMS IN LASER POWDER BED FUSION

Current problems

- Substantial structure defects, e.g. porosity, cracks, etc
- High-fidelity models to capture all physics
- Build repeatability and reliability (particularly fusion based AM)

Challenges for characterization

- Defects are underneath surface
- Complex energy-matter interaction and mass/heat flow
- Multiscale structures and dynamics

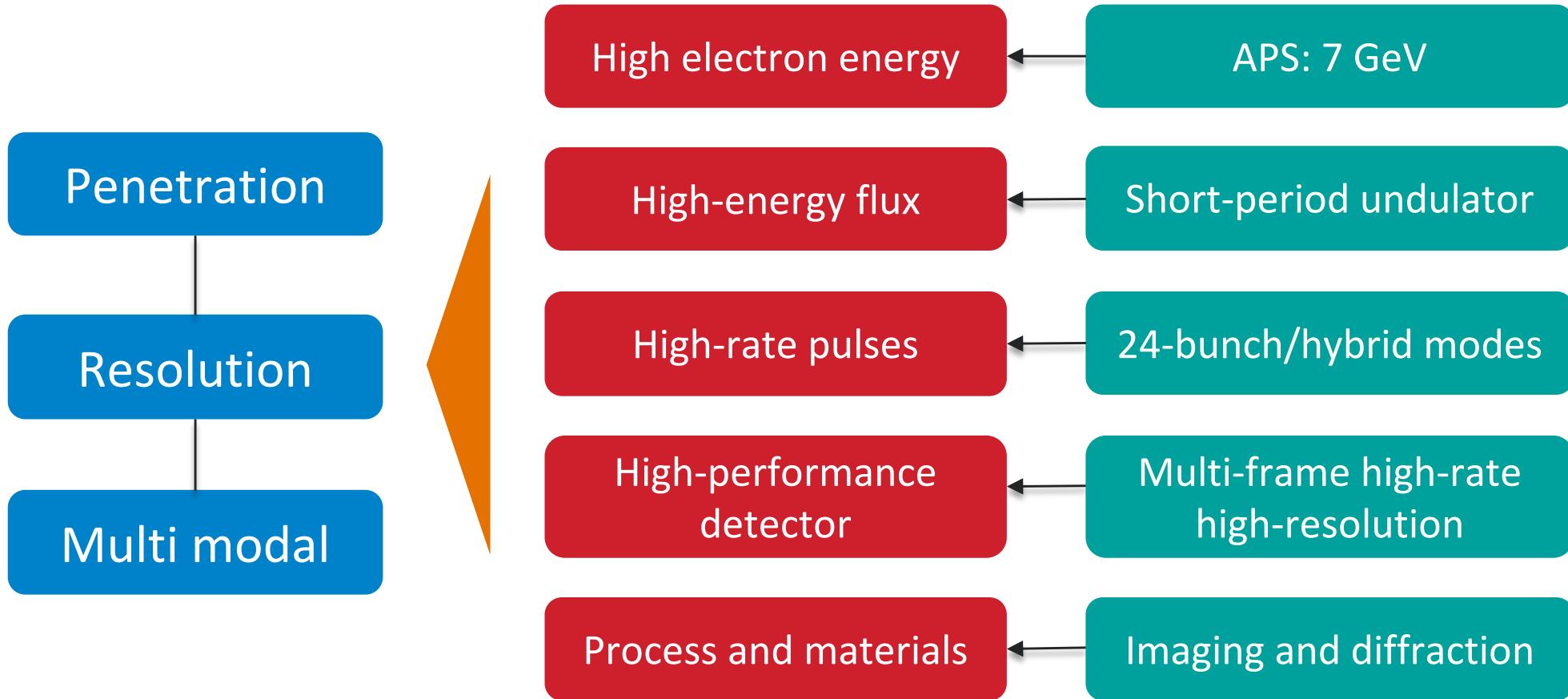


M. Wang, et al., Nature Materials, 17, (2018) 63

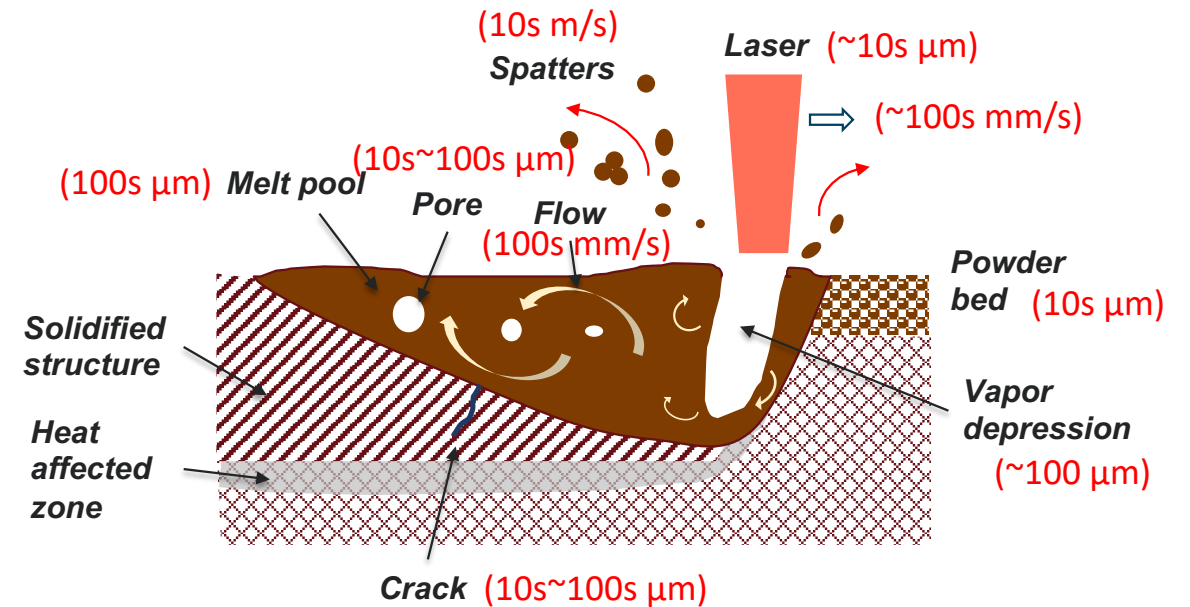
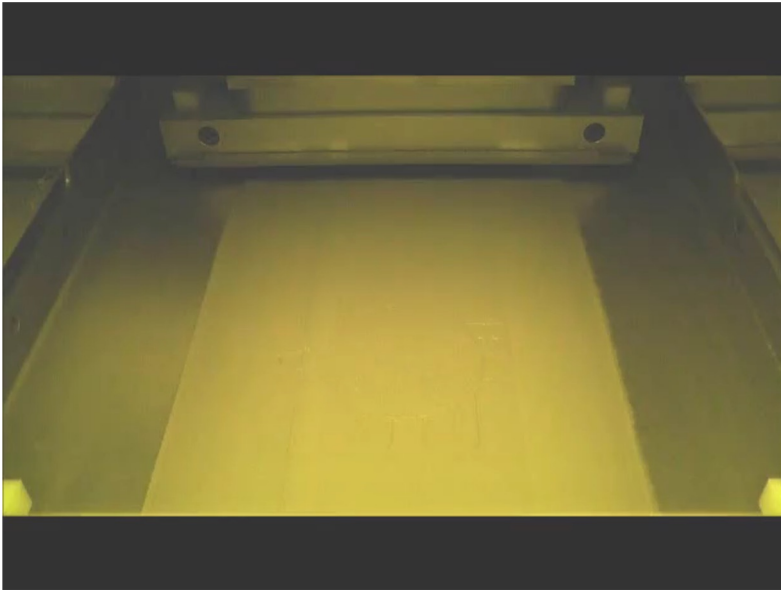
D. Gu, et al., International Materials Reviews, 57, (2012) 133

WHY X-RAY, WHY SYNCHROTRON, WHY APS

Advanced Photon Source: 3rd-generation high-energy synchrotron facility



LASER POWDER BED FUSION



Highly dynamic processes induced by the extreme thermal conditions

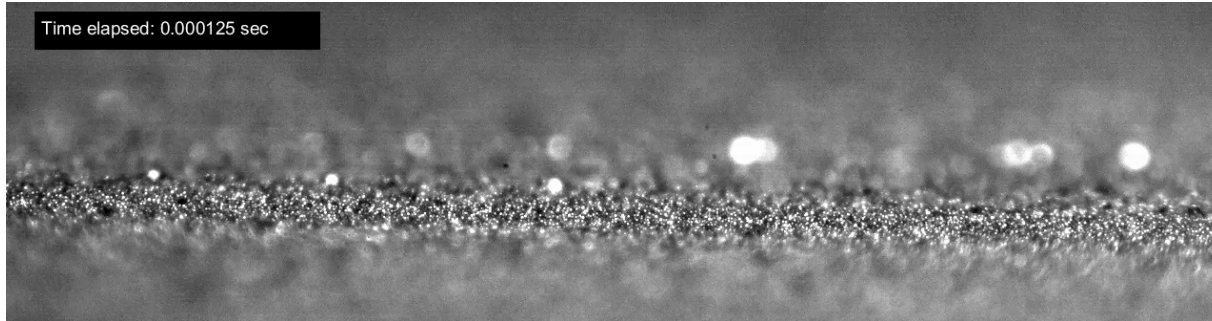
- High temperature: beyond boiling temperature
- High heating and cooling rates: $10^5 - 10^7$ K/s
- Large thermal gradient: $10^3 - 10^7$ K/mm
- Short laser-metal interaction time: $\mu\text{s} - \text{ms}$

Phenomena

- Melting and vaporization of metal
- Melt flow inside the melt pool
- Particle spattering and powder entrainment
- Oscillation of melt pool and vapor depression zone
- Rapid solidification and phase transformation

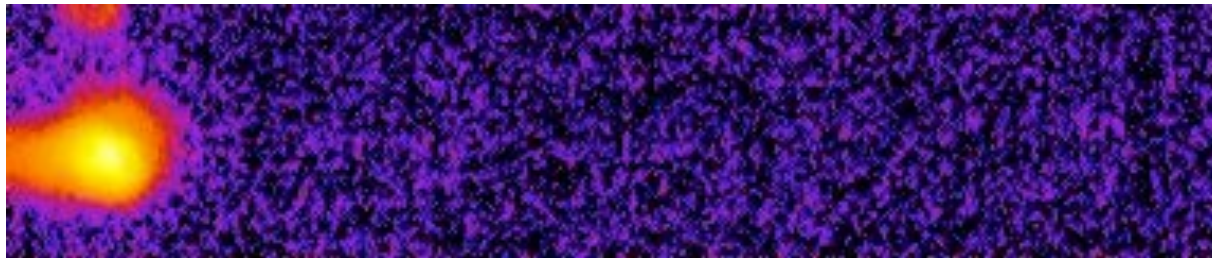
REAL-TIME MONITORING AND SENSING OF LPBF

High-speed visible-light imaging



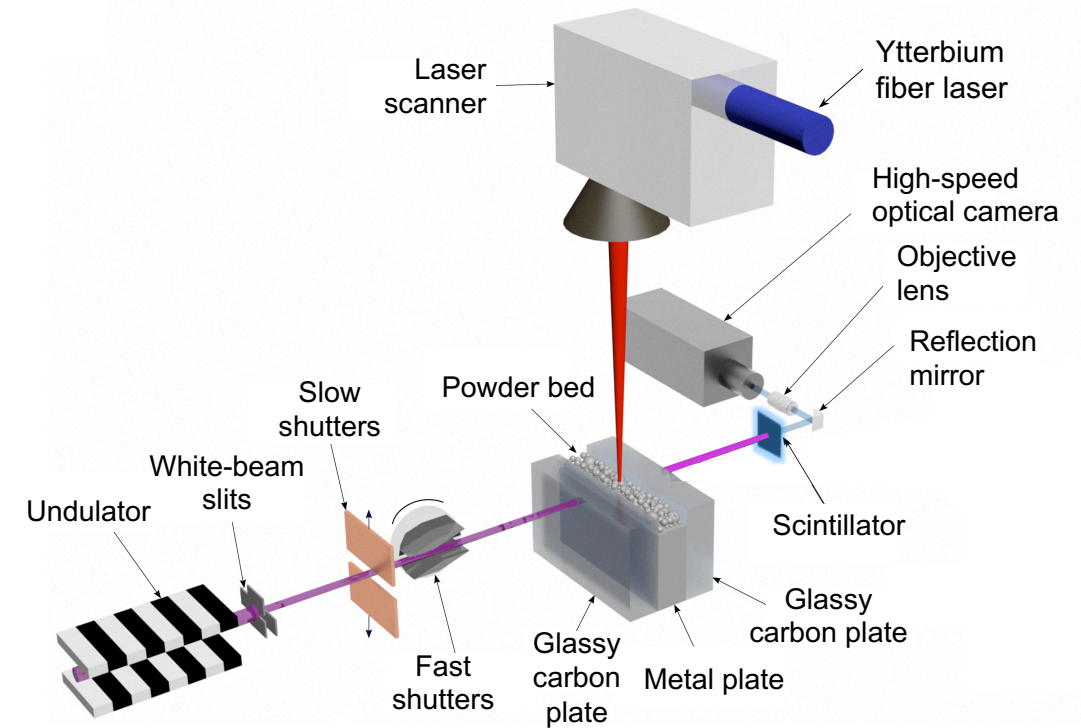
P.Bidare, et a., Acta Materialia, 142, (2018), 107-120

High-speed near infrared imaging

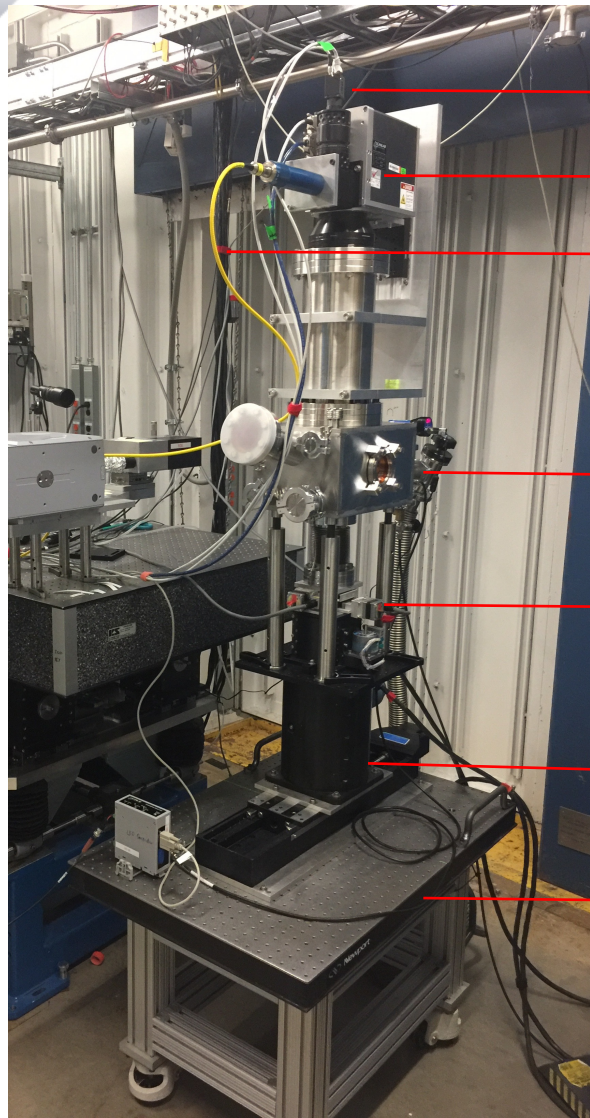


Unpublished

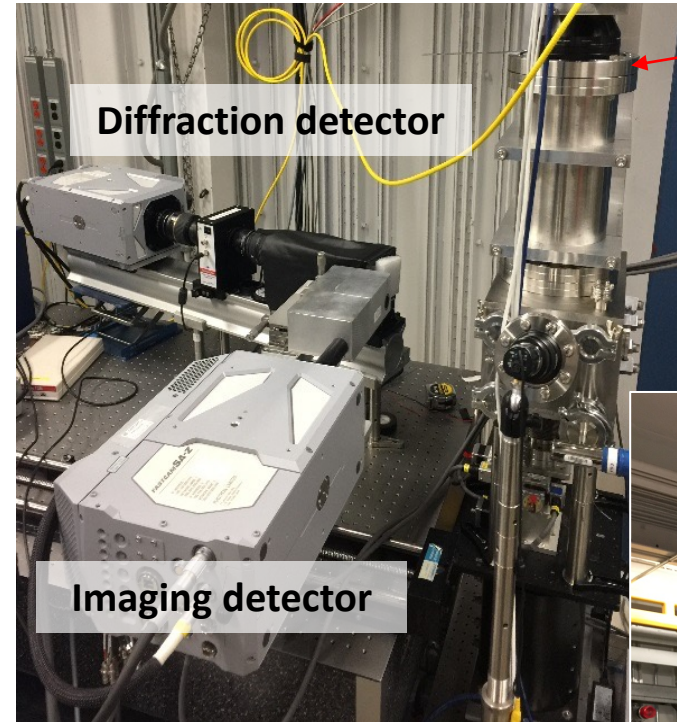
Synchrotron x-ray imaging



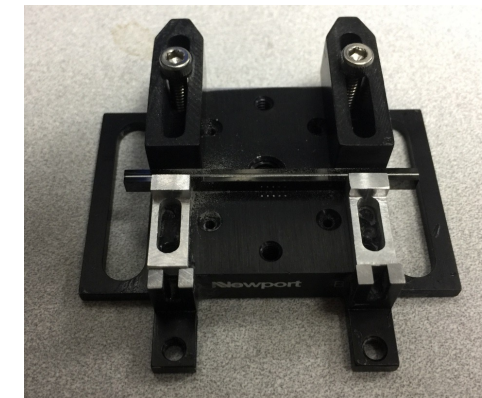
LASER POWDER BED FUSION EXPERIMENT AT APS



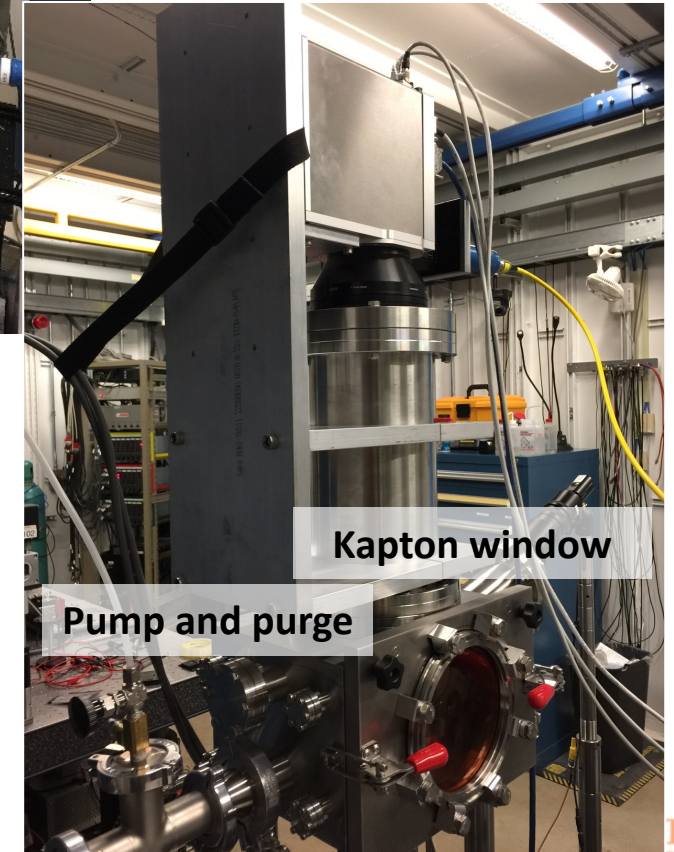
- Top view camera
- Laser scanner
- Fiber laser
- Sample chamber
- Sample motor stack
- Chamber motors
- Optic table with casters



Fused silica laser entrance window



Sample



Kapton window

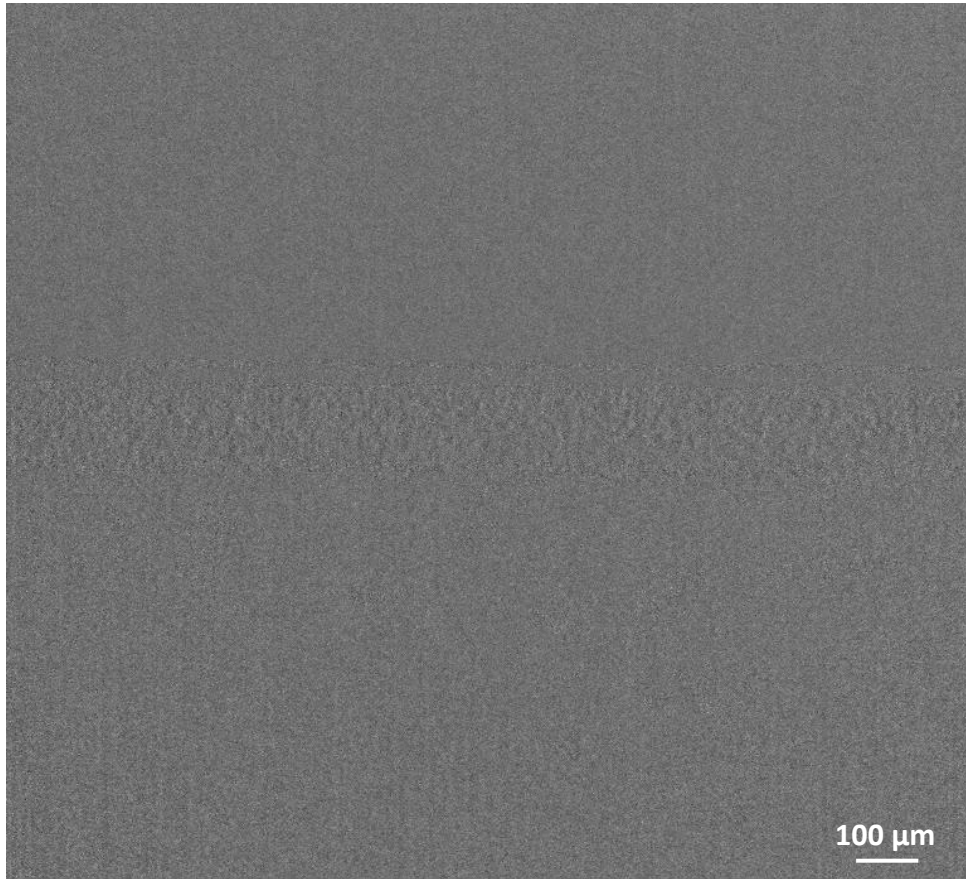
Pump and purge

C. Zhao, et al., Scientific Reports, 7, (2017) 3602

N. Parab, C. Zhao, et al., J. Synchrotron Radiation, 25, (2018) 1467

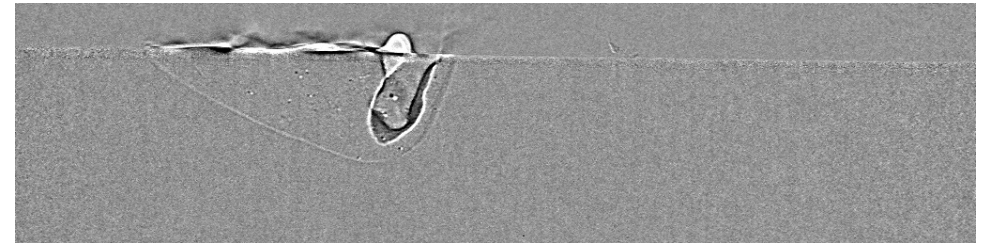
X-RAY VISION OF LASER POWDER BED FUSION

Simple ImageJ data processing to highlight melt pool boundary

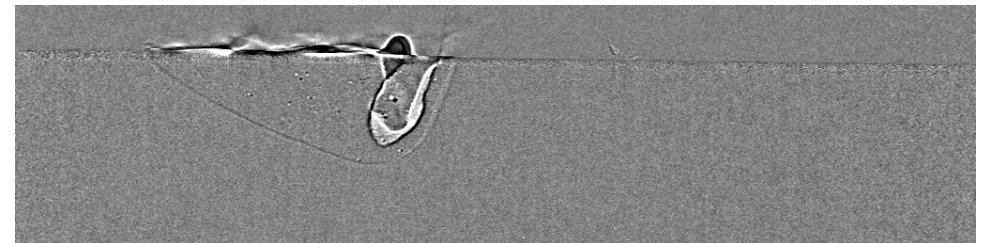


- Material: Al-10Si-Mg
- Laser power: 520 W
- Scan speed: 0.6 m/s
- Recording rate: 30,173 fps
- Exposure: 0.1 ns
- Pixel resolution: 2 μm

I1 = Frame 1 / Frame 2



I2 = Frame 2 / Frame 1

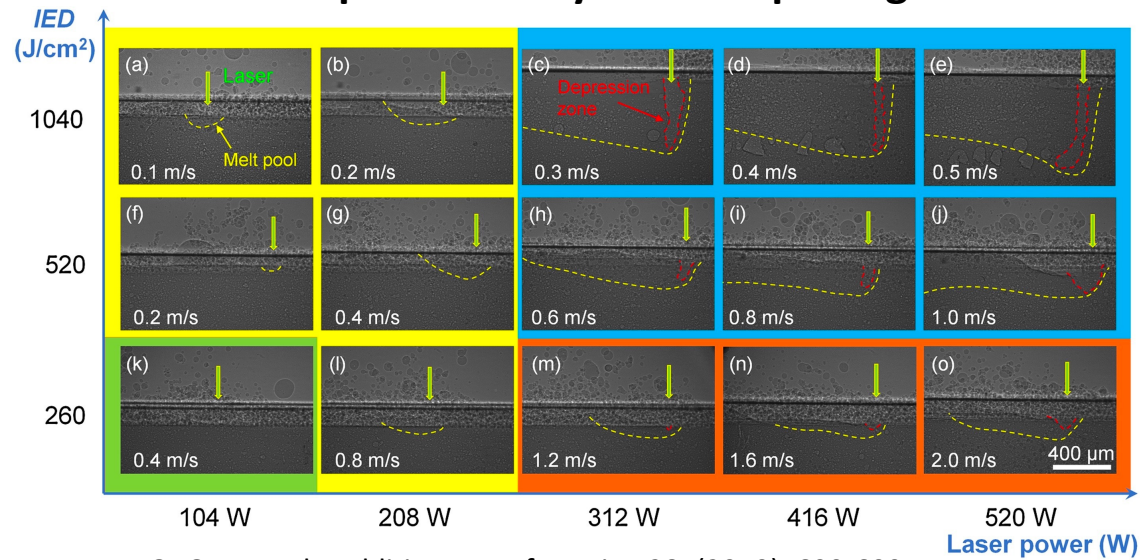


Max (I1,I2), then despeckle



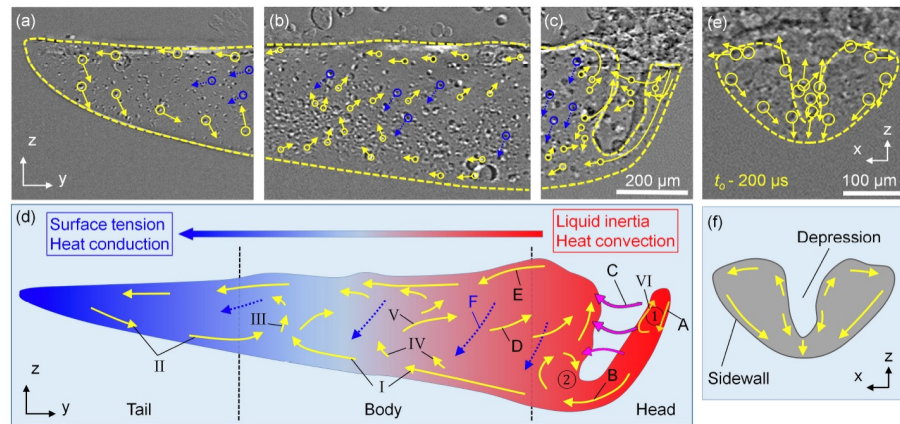
QUANTITATIVE MEASUREMENTS

Melt pool and keyhole morphologies



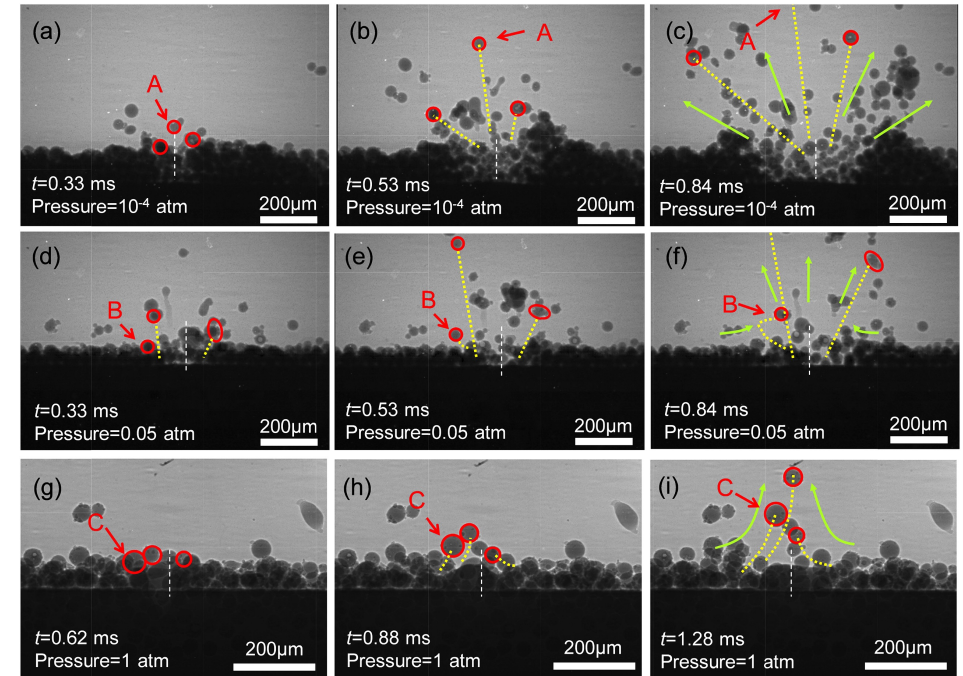
Q. Guo, et al., Additive Manufacturing 28, (2019), 600-609

Melt flow



Q. Guo, et al., Additive Manufacturing, 31, (2020), 100939

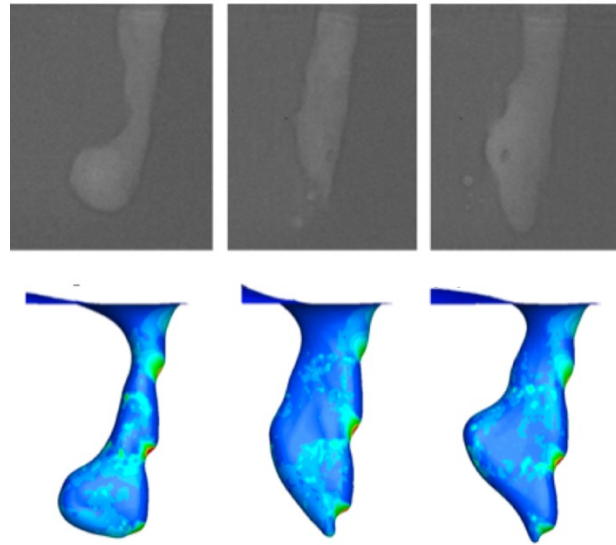
Particle spattering



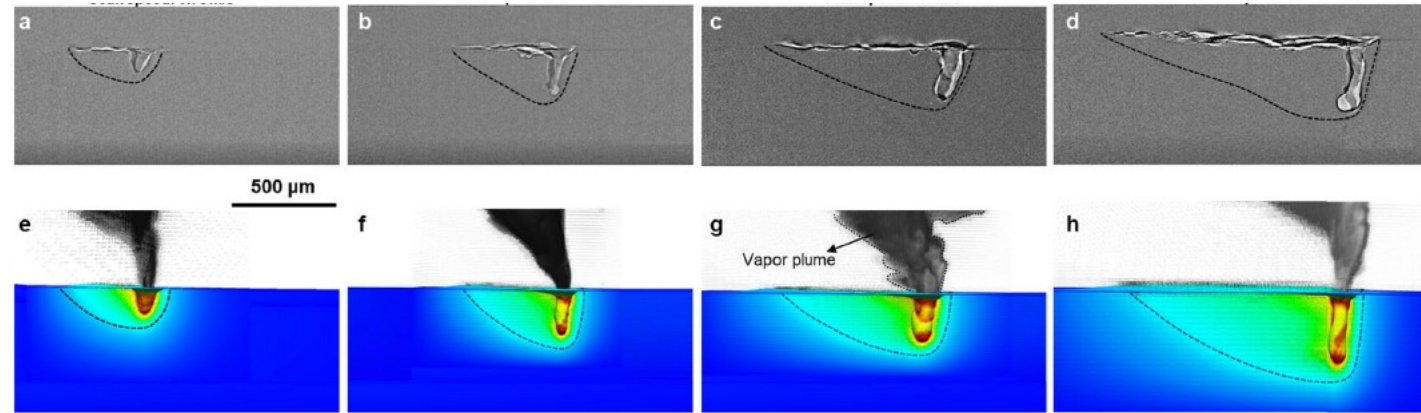
Q. Guo, C. Zhao, et al., Acta Materialia, 151, (2018) 169-180

Collaboration with Lianyi Chen at
University of Wisconsin-Madison

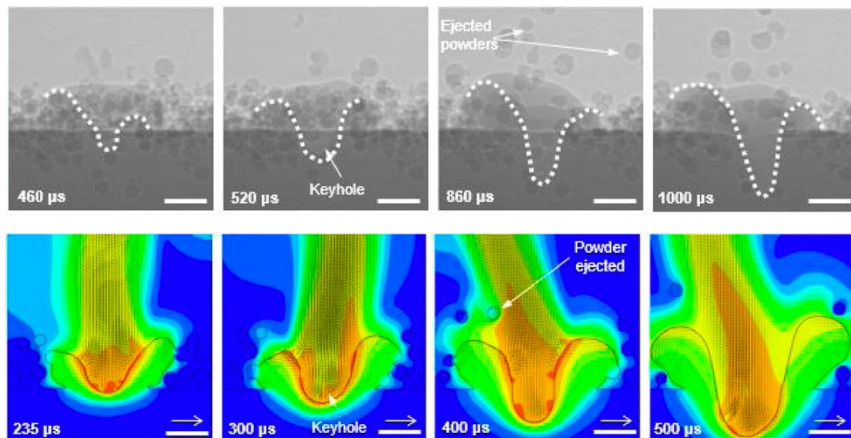
CALIBRATE AND VALIDATE MODELS



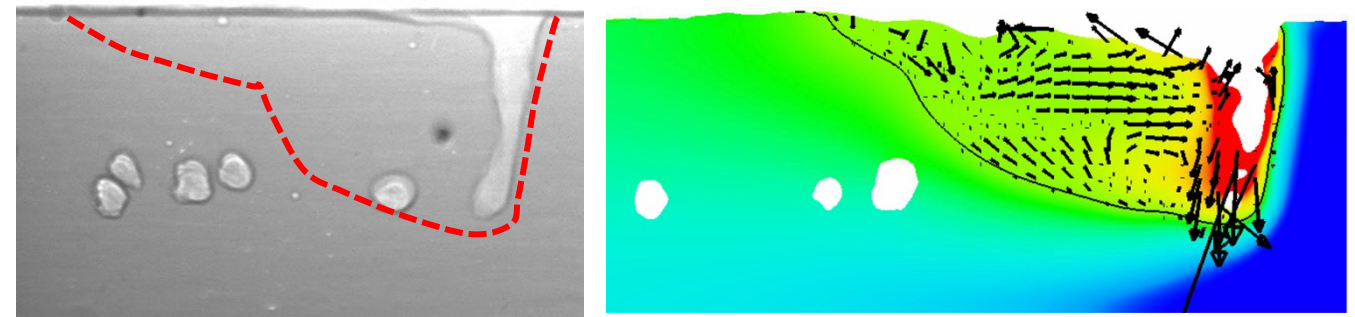
N. Kouraytem, et al., Physical Review Applied 11, (2019), 064054



Z. Gan, et al., Nature Communications, 12, (2021) 2379



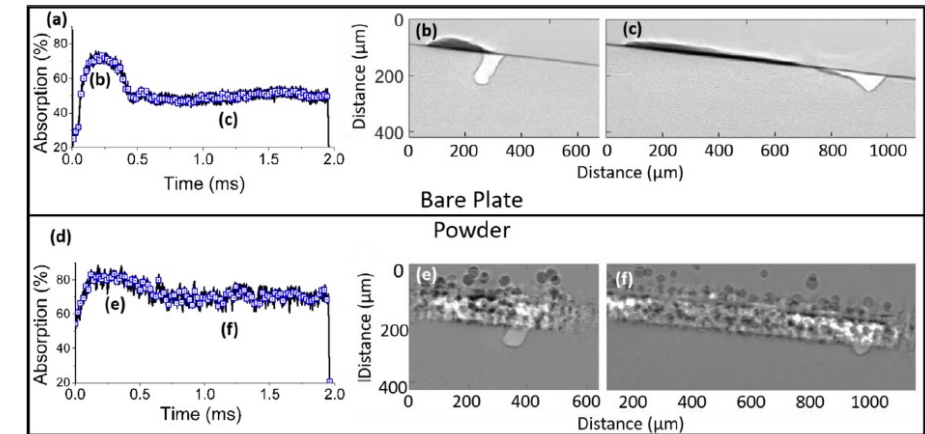
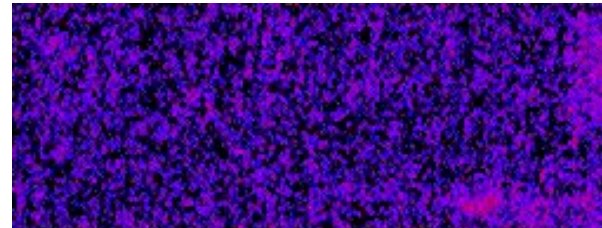
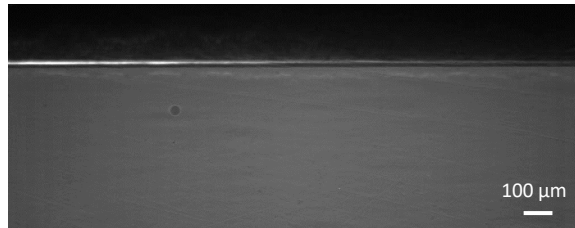
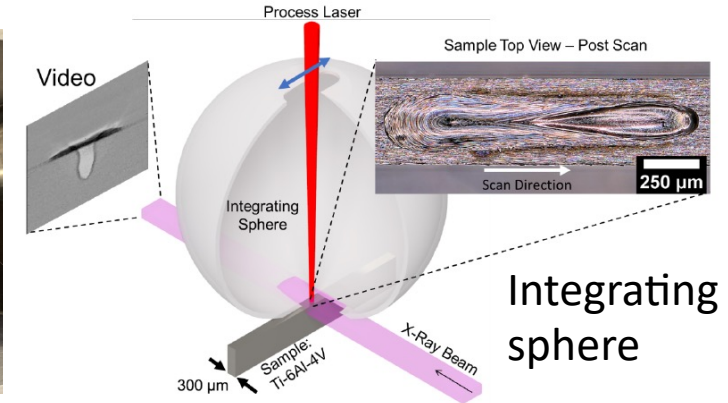
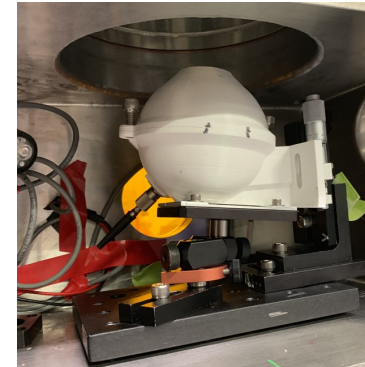
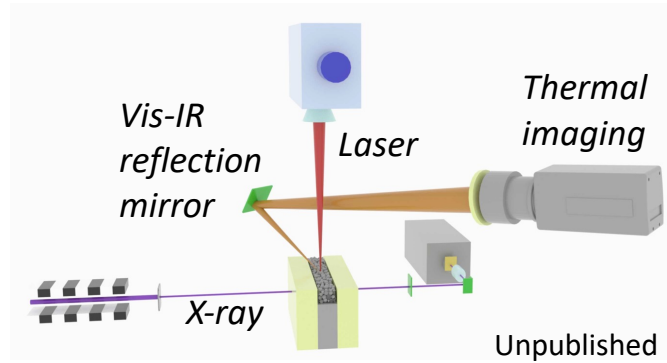
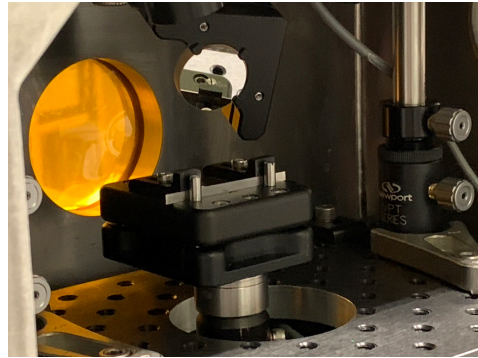
X. Li, et al., Additive Manufacturing, 35, (2020) 101362



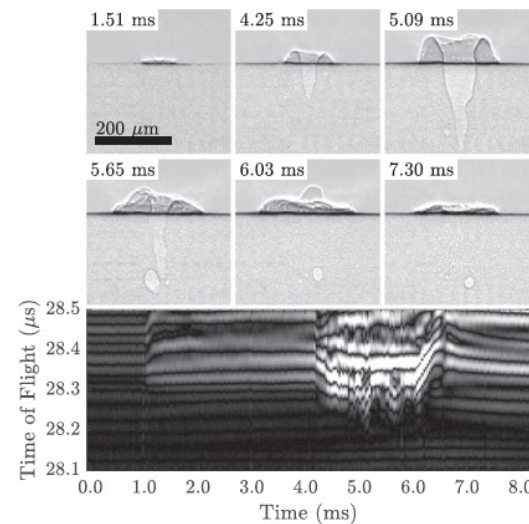
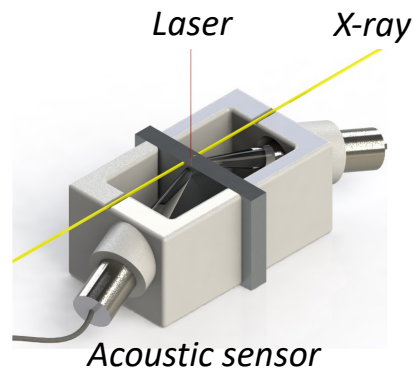
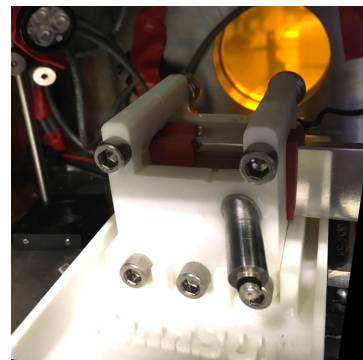
unpublished

Collaboration with Wenda Tan at University of Michigan, and Wing Kam Liu and Zhengtao Gan at Northwestern University

MULTI-MODAL SENSING



B. Simonds, et al., Applied Materials Today 23 (2021) 101049



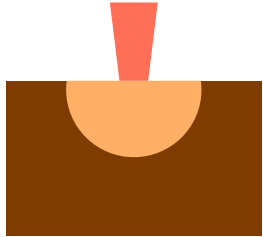
J. Gillespie, et al., Journal of Acoustic Society of America, 150, (2021) 2409

Collaboration with Brian Simonds at NIST, and Christopher Kube at Penn State University

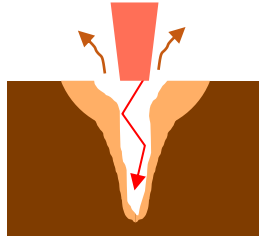
DYNAMICS OF VAPOR DEPRESSION

Laser melting modes

Conduction

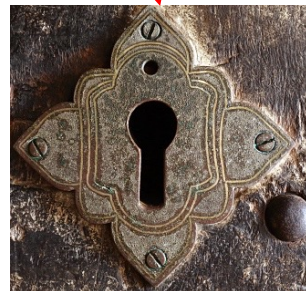
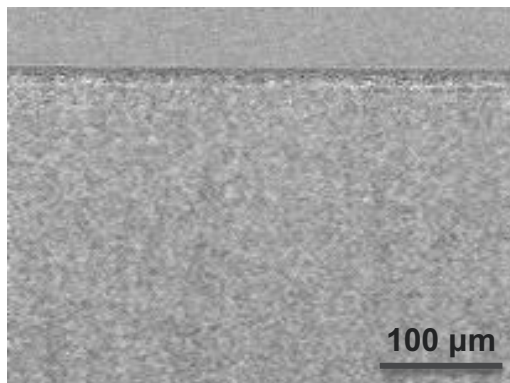
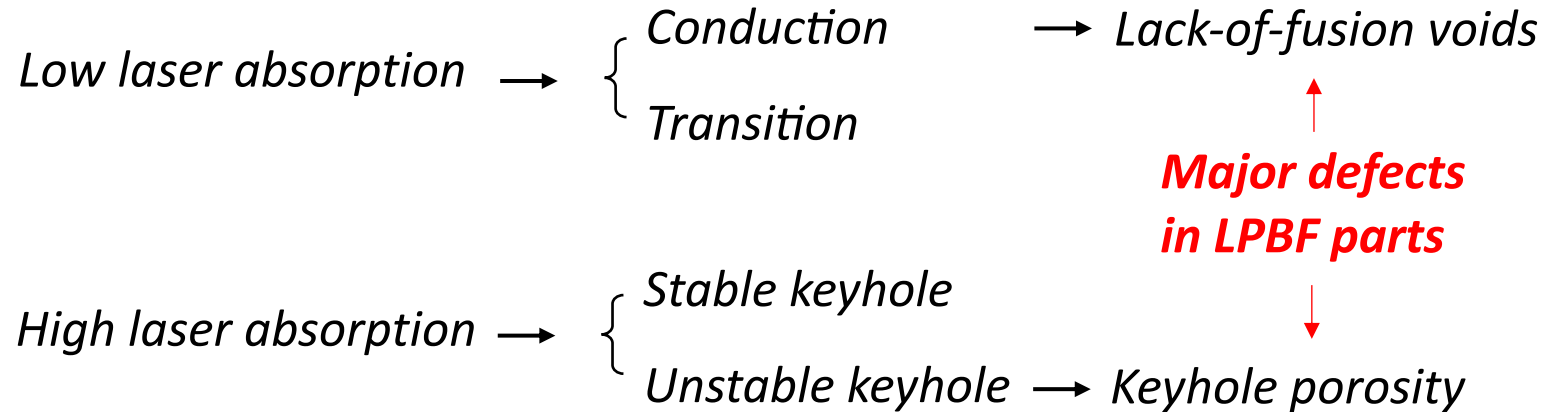


Keyhole



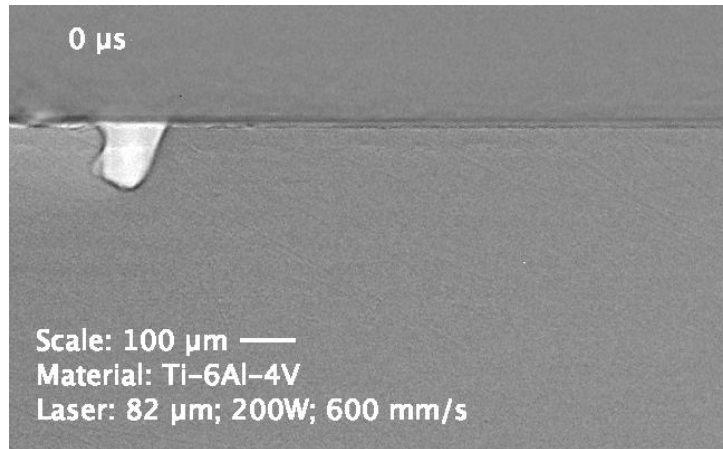
Why study keyhole?

- I. Keyhole connects energy coupling efficiency, melting mode, and defects
- II. Keyhole cannot be directly visualized using other techniques

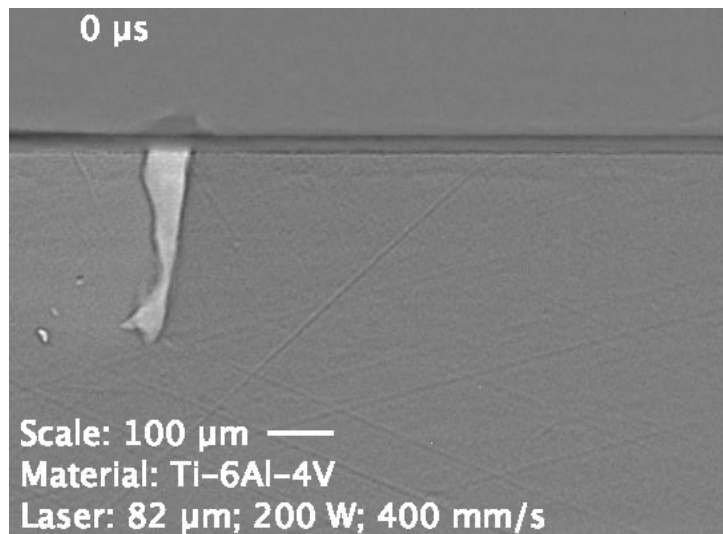


KEYHOLE DYNAMICS AND FUNDAMENTAL PHYSICS IN LPBF

Stable keyhole



Unstable keyhole

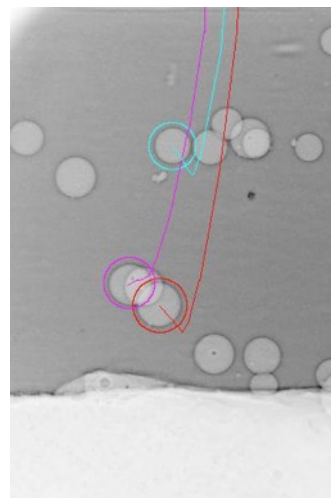
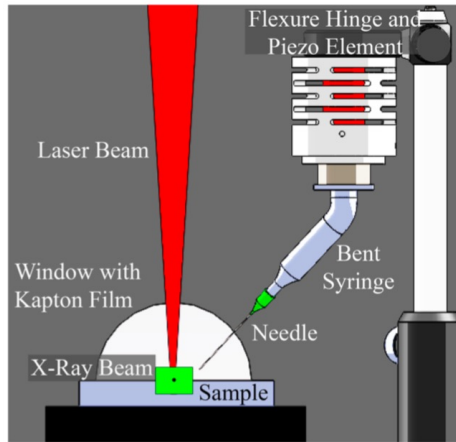


Further reading

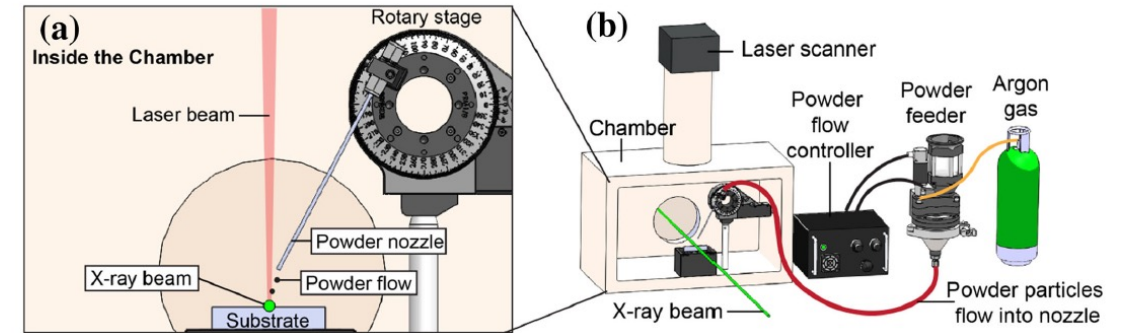
- C. Zhao, N. Parab, X. Li, K. Fezzaa, W. Tan, A. Rollett, T. Sun, “Critical instability at moving keyhole tip generates porosity in laser melting”, *Science*, 370, (2020) 1080
- C. Zhao, Q. Guo, X. Li, N. Parab, K. Fezzaa, W. Tan, L. Chen, T. Sun, “Bulk explosion induced metal spattering during laser processing”, *Physical Review X*, 9, (2019) 021052
- R. Cunningham*, C. Zhao*, N. Parab, K. Fezzaa, T. Sun, A. Rollett, “Keyhole Threshold and Morphology in Laser Melting Revealed by Ultrahigh-Speed X-ray Imaging”, *Science*, 363, (2019) 849 (*equal contribution)
- S. Hojjatzadeh, N. Parab, W. Yan, Q. Guo, L. Xiong, C. Zhao, L. Escano, M. Qu, X. Xiao, K. Fezzaa, W. Everhart, T. Sun, L. Chen, “Mechanisms of pore elimination during 3D printing of metals”, *Nature Communications*, 10, (2019) 3088
- Z. Gan, O. Kafka, N. Parab, C. Zhao, L. Fang, O. Heinonen, T. Sun, and WK. Liu, “Universal scaling laws of keyhole stability and porosity in 3D printing of metals”, *Nature Communications*, 12, (2021) 2379
- I. Bitharas, N. Parab, C. Zhao, T. Sun, A.D. Rollett and A.J. Moore, “The interplay between vapour, liquid, and solid phases in laser powder bed fusion”, *Nature Communications*, 13, (2022), 2959
- S. Khairallah, T. Sun, B. Simonds, “Onset of periodic oscillations as a precursor of a transition to pore-generating turbulence in laser melting”, *Additive Manufacturing Letters*, 1, (2021) 100002
- B. Simonds, J. Tanner, A. Artusio-Glimpse, P. Williams, N. Parab, C. Zhao, **T. Sun**, “The Causal Relationship between Melt Pool Geometry and Energy Absorption Measured in Real Time During Laser-Based Manufacturing”, *Applied Materials Today*, 23, (2021) 101049

POWDER-FEED DIRECTED ENERGY DEPOSITION

Gravity-feed

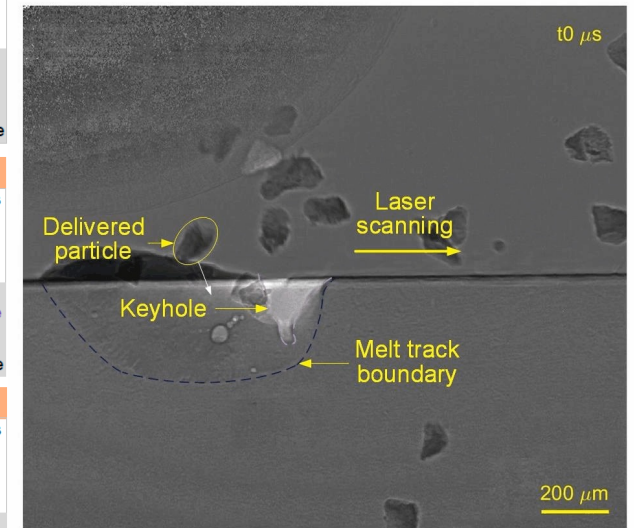


Blown-powder



A few generations of operando DED systems

Pores inside particle	Pores from particle top surface	Pores entrapped by particle bottom
Keyhole pores (Type I)	Keyhole pores (Type II)	Keyhole pores (Type III)
Lack of fusion of the particle	Particle movement in the melt pool	Pores induced by inert gas



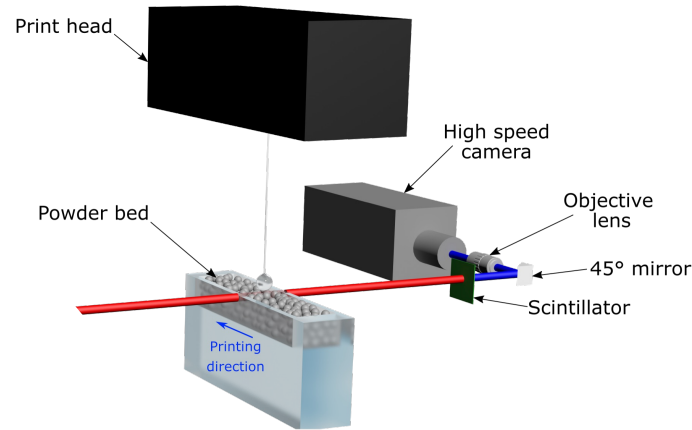
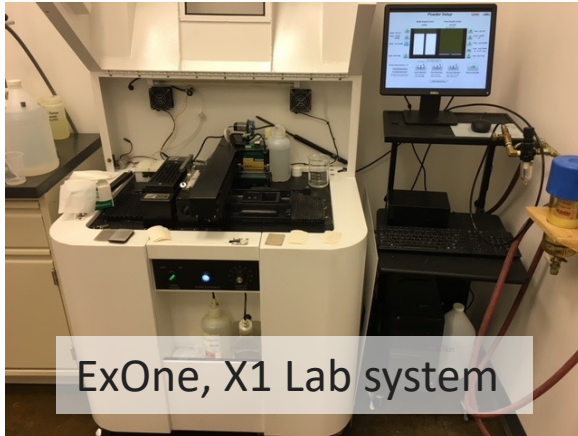
S. Wolff, et al., Scientific Reports. 9, (2019) 962

Collaboration with Dr. Sarah Wolff at TAMU and Dr. Jian Chao at Northwestern

S. Wolff, et al., International Journal of Machine Tools and Manufacture, 166, (2021) 103743

S. Wolff*, S. Webster*, et al., JOM, 73, (2021) 189

BINDER JETTING

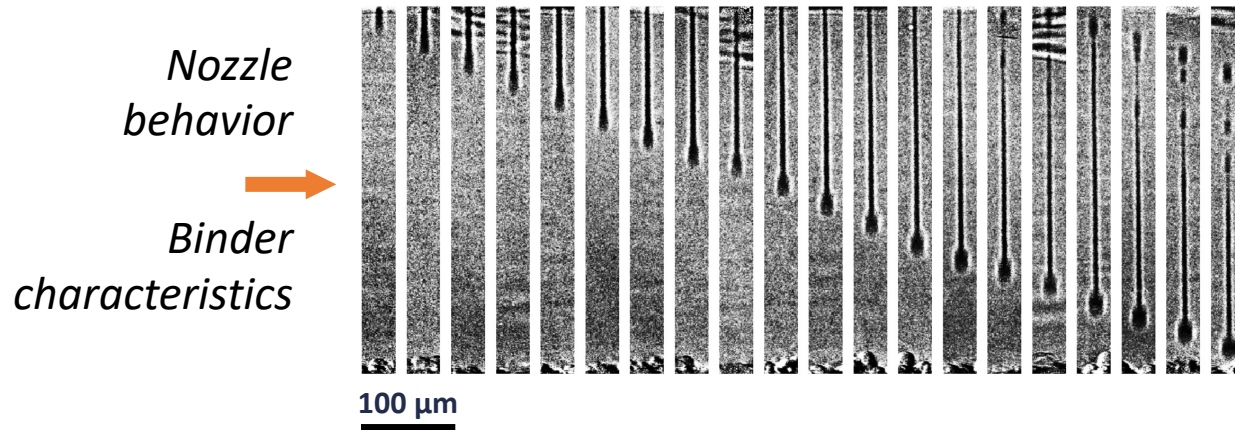


SS316, spherical, 30 μm

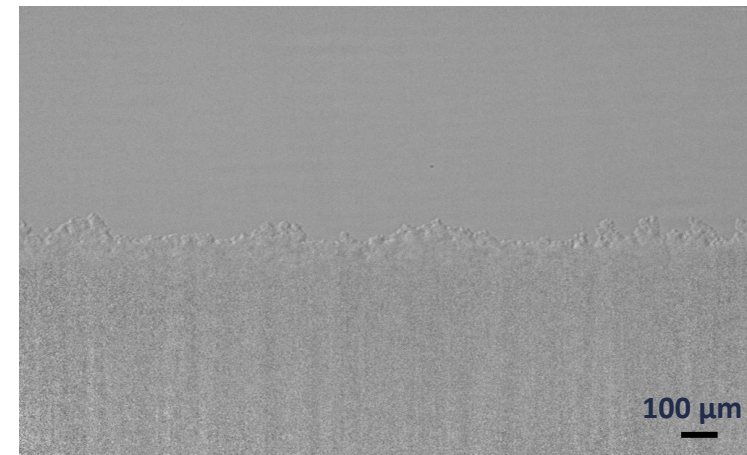


← Powder ejection
← Powder depletion layer

Binder droplet dynamics



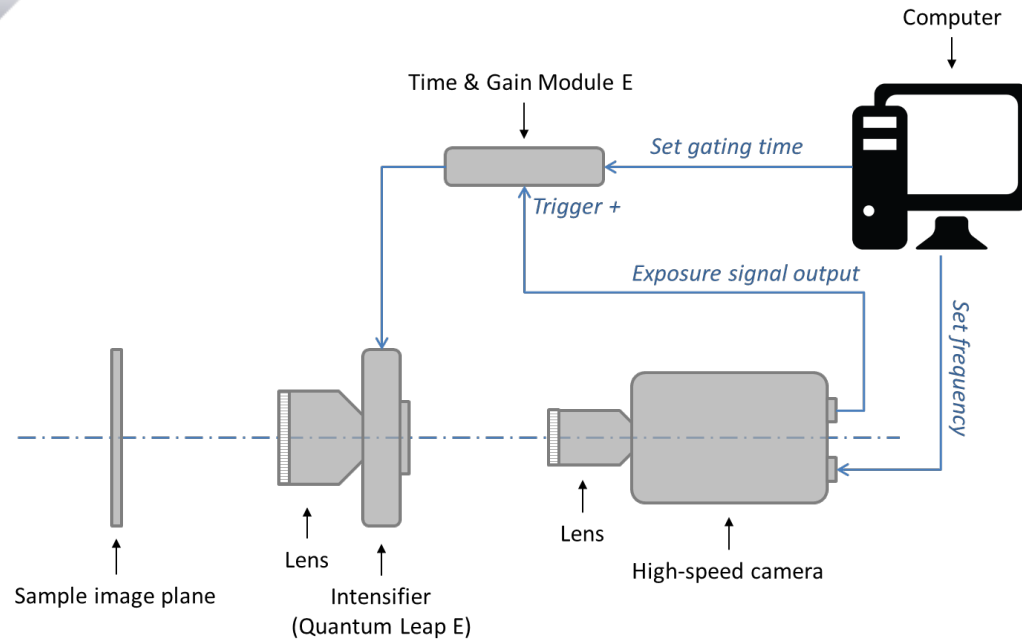
SS316, spherical, 9 μm



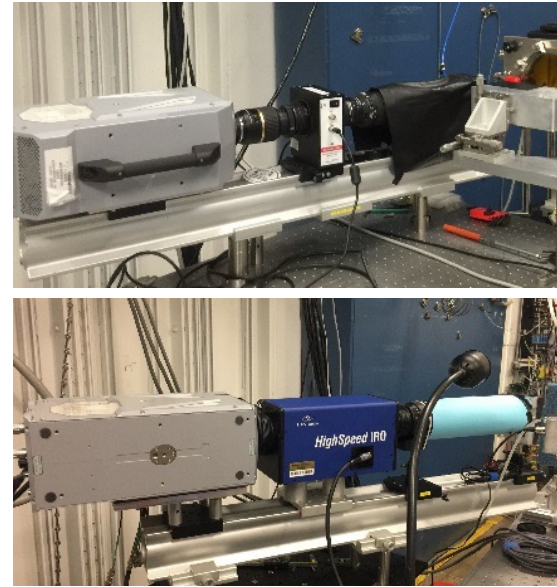
← Balling

Collaboration with John Barnes at TBGA, Dan Brunemer at ExOne, and Tony Rollett at CMU

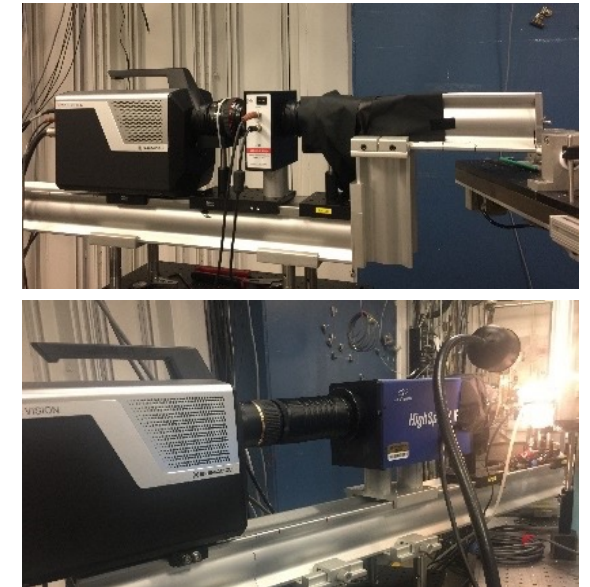
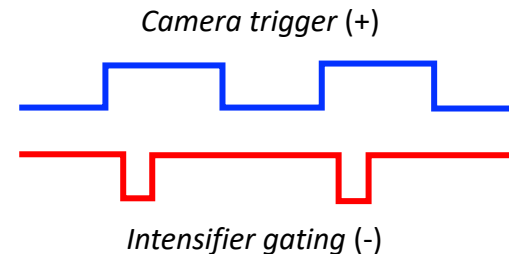
HIGH-SPEED DIFFRACTION DETECTION SYSTEMS AT 32-ID



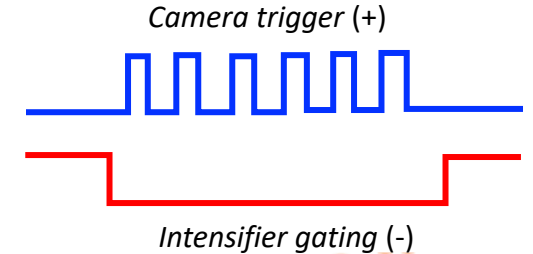
- ❑ **Intensifier:** LaVision IRO, Quantum Leap
- ❑ **Camera:** Photron SA-Z, Shimadzu HPV-X2
- ❑ **Scintillator:** $\text{Lu}_{1.8}\text{Y}_{0.2}\text{SiO}_5:\text{Ce}$ (LYSO)
 - Thickness: 300 μm
 - Diameter: 65 mm
 - Al front coating



- Camera: Photron SA-Z
- Intensifier trigger: multiple
- Pixels: 1024 x 1024 (60~70 $\mu\text{m}/\text{pixel}$)
- Min exposure: 100 ps
- Max frame rate: 200 kHz
- Fast dynamics spanning 10s' ms

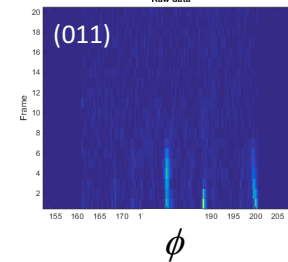
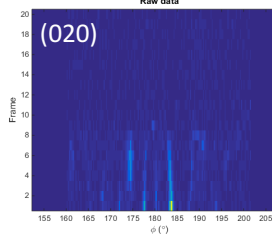
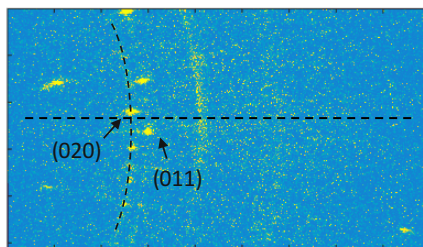
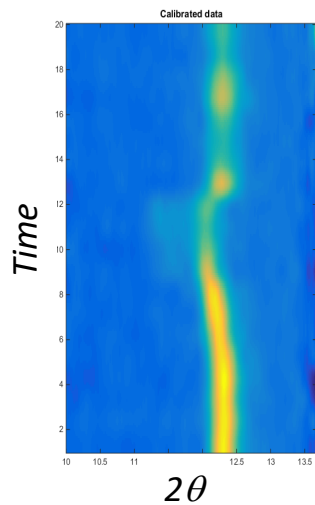
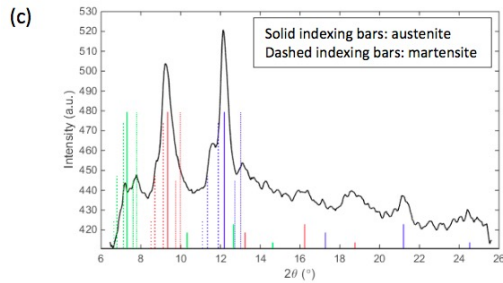
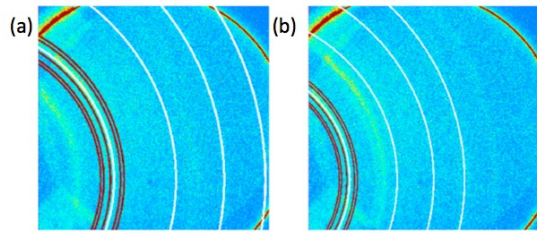


- Camera: Shimadzu HPV-X2
- Intensifier trigger: single
- Pixels: 400 x 250 (60~70 $\mu\text{m}/\text{pixel}$)
- Min exposure: 100 ps
- Max frame rate: 10 MHz
- Ultrafast dynamics spanning 10s' μs



DATA ANALYSIS SOFTWARE

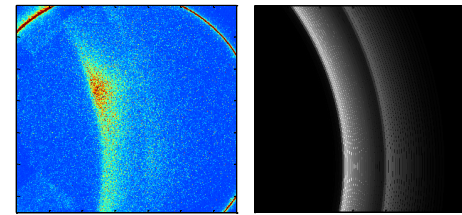
HiSPoD: High-Speed Polychromatic Diffraction



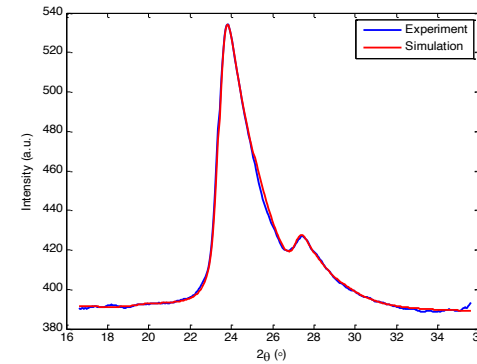
Indexing

Simulation

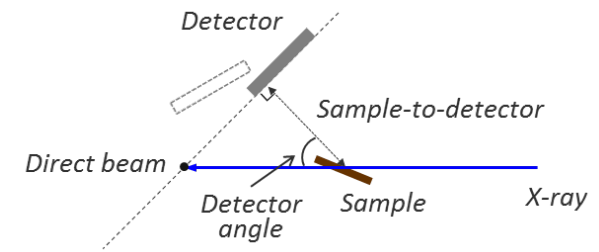
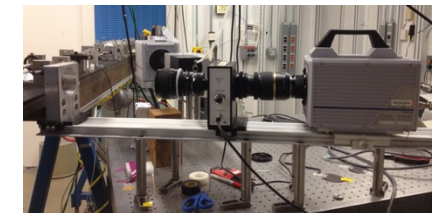
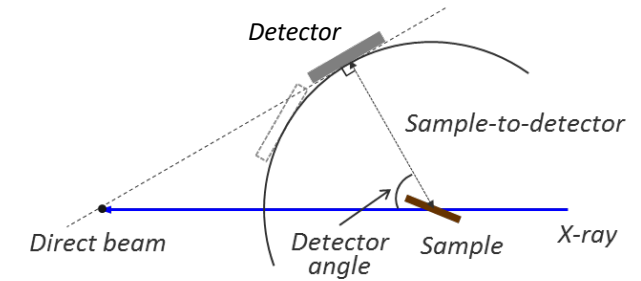
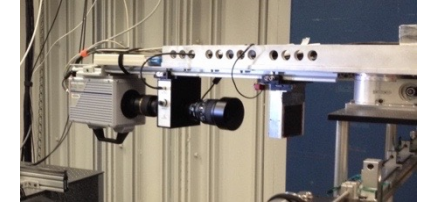
Intensity integration



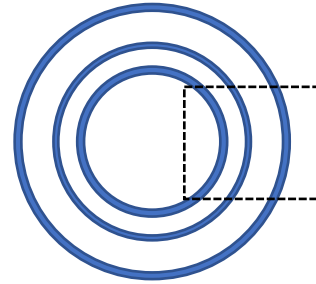
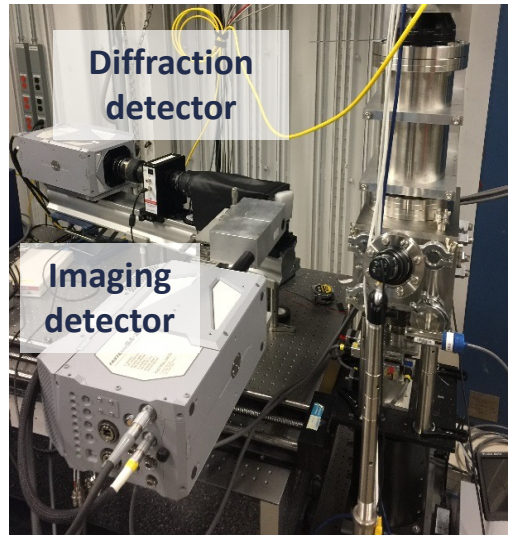
$$I_{white} = \int_{E_1}^{E_2} \left(\sum_{i=1}^n I_{hkl_i}(\theta, E) \right) \cdot F(E) dE$$



Scattering geometry

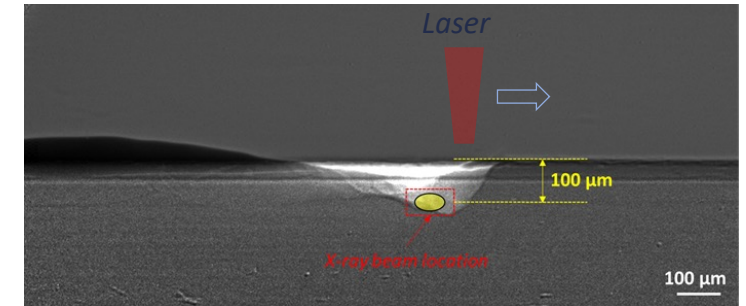


PINK BEAM DIFFRACTION AT 32-ID

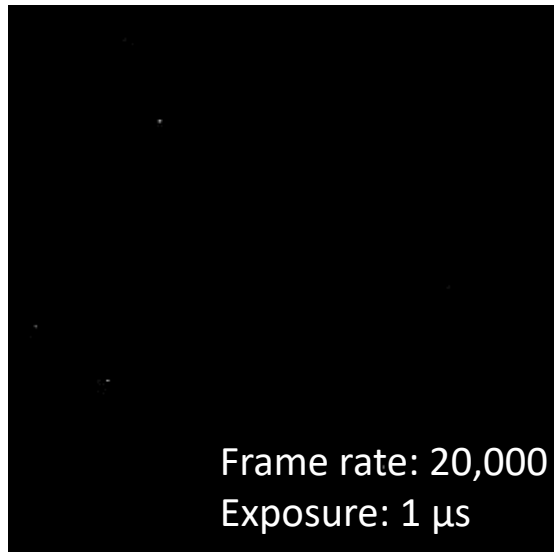
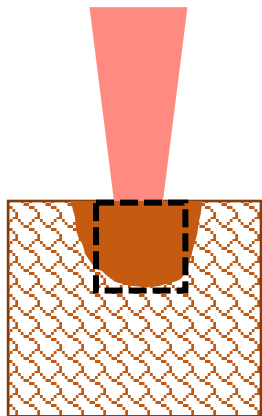


- ❑ Phase transformation of Ti-6Al-4V
 α -Ti \rightarrow melting \rightarrow β -Ti with coarse grains \rightarrow α -Ti with fine grains
- ❑ 32-ID source
 - U18 pink: ~ 24 keV (1st)
 - Bandwidth: $\sim 5\%$
- ❑ Detector
 - Scintillator + intensifier + optical CMOS camera

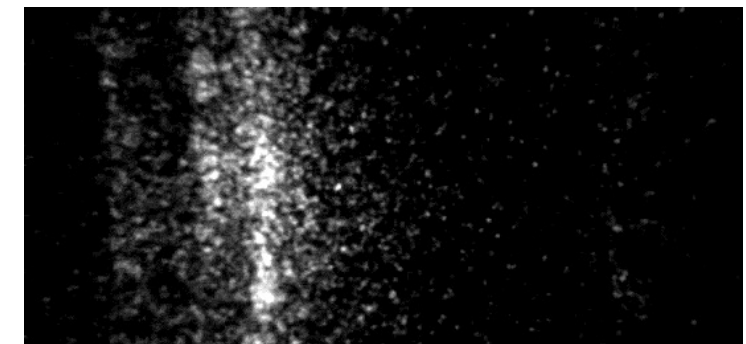
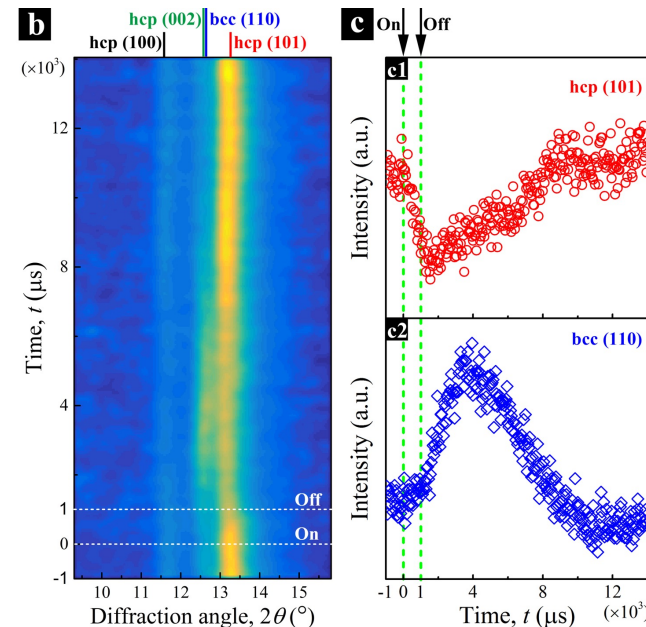
Scanning laser mode



Spot welding mode

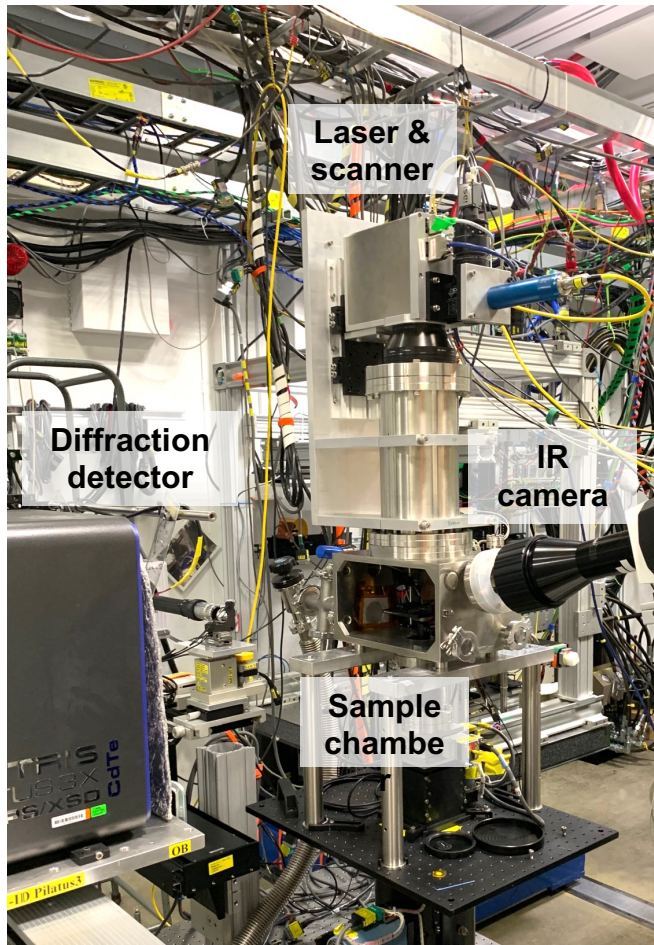


C. Zhao, et al., Scientific Reports, 7, (2017) 3602



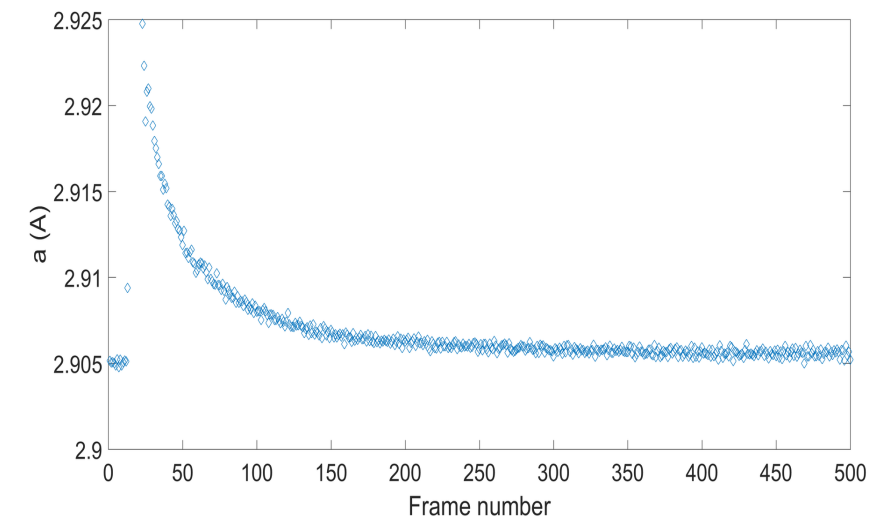
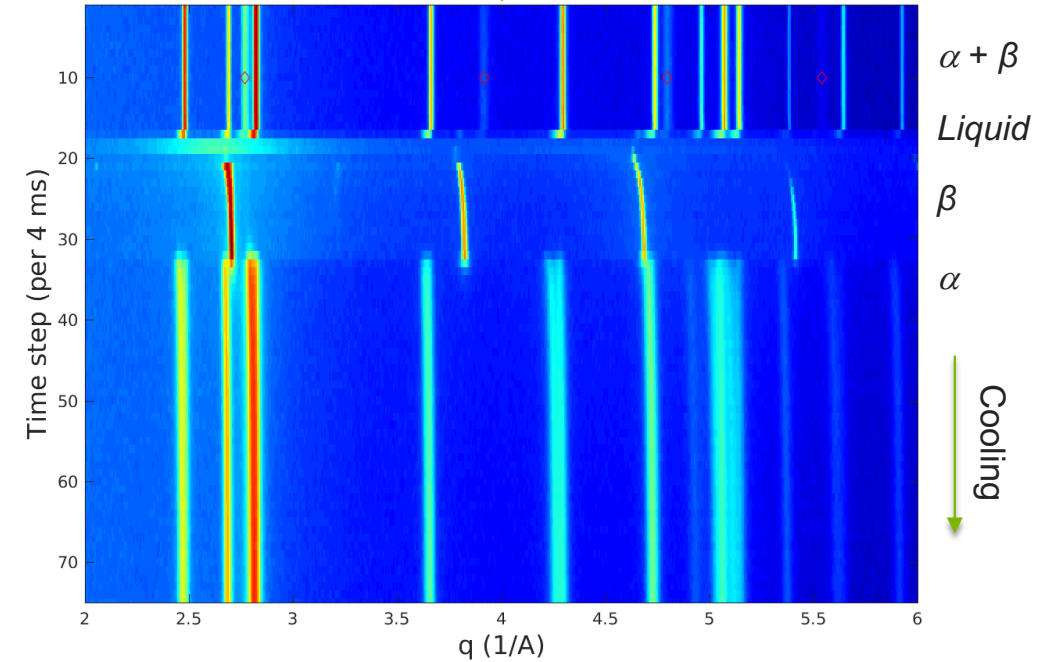
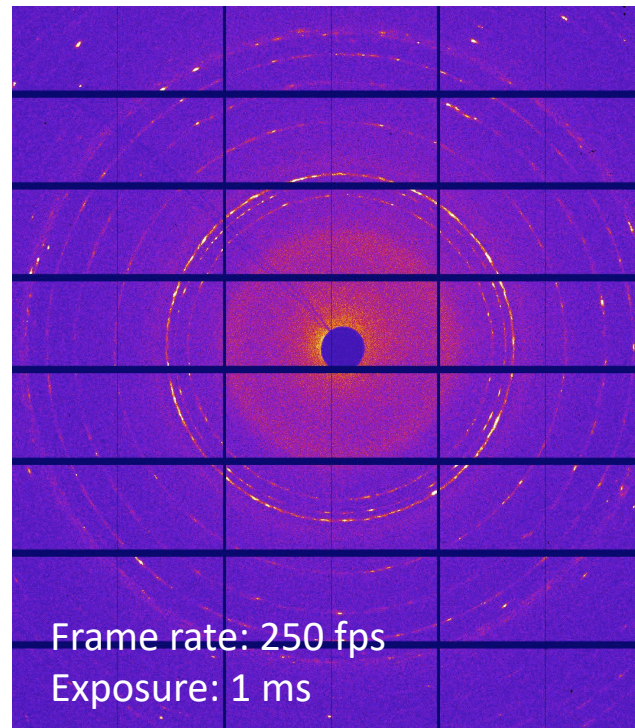
Frame rate: 100,000 fps
 Exposure: 5 μ s
 X-ray beam size: H100 x V60 μ m²

MONO BEAM DIFFRACTION AT 1-ID



(with Andrew Chuang, APS)

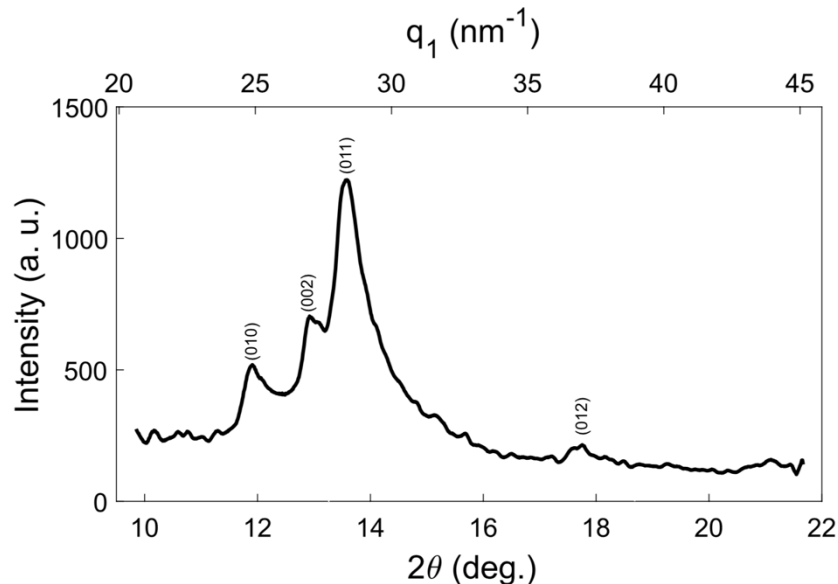
- ❑ 1-ID source
 - Superconducting undulator
 - Mono: $E = 55.6$ keV
- ❑ Detector
 - PILATUS3X 2M CdTe



S. Oh, et al., Materials Research Letters, 9, (2021) 429

COMPARISON OF IN SITU DIFFRACTION DATA

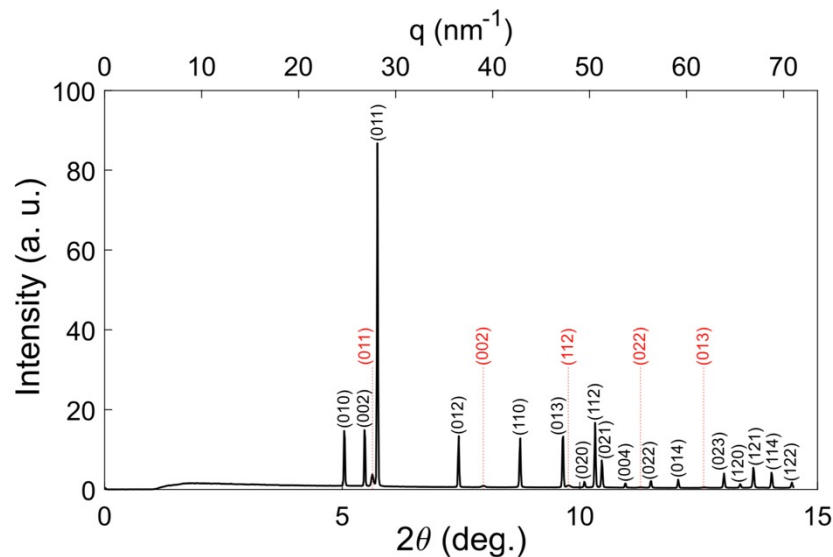
32-ID
pink beam



- X-ray energy: mid-energy pink beam
- Detector: small indirect detection
- Frame rate: 100s' kHz
- Exposure time: microsecond
- Detector dynamic range: low
- S/N: low

Fast, but limited detection

1-ID
mono beam



- X-ray energy: high-energy mono beam
- Detector: large direct detection
- Frame rate: 100s Hz
- Exposure time: millisecond
- Detector dynamic range: high
- S/N: high

Slow, but high resolution

FEEDBACK

Lecture: 9:45 – 10:45 (Jul. 19, 2022)

Fast x-ray imaging and diffraction for engineering materials science - Tao Sun

<https://forms.office.com/g/X8Esg0WPvJ>

